

Electroweak Baryogenesis and Dark Matter with an approximate R -symmetry

Piyush Kumar and Eduardo Pontón

Department of Physics & ISCAP

538 W 120th street

Columbia University, New York, NY 10027

Abstract

It is well known that R -symmetric models dramatically alleviate the SUSY flavor and CP problems. We study particular modifications of existing R -symmetric models which share the solution to the above problems, *and* have interesting consequences for electroweak baryogenesis and the Dark Matter (DM) content of the universe. In particular, we find that it is naturally possible to have a strongly first-order electroweak phase transition while simultaneously relaxing the tension with EDM experiments. The R -symmetry (and its small breaking) implies that the gauginos (and the neutralino LSP) are pseudo-Dirac fermions, which is relevant for both baryogenesis and DM. The singlet superpartner of the $U(1)_Y$ pseudo-Dirac gaugino plays a prominent role in making the electroweak phase transition strongly first-order. The pseudo-Dirac nature of the LSP allows it to behave similarly to a Dirac particle during freeze-out, but like a Majorana particle for annihilation today and in scattering against nuclei, thus being consistent with current constraints. Assuming a standard cosmology, it is possible to simultaneously have a strongly first-order phase transition conducive to baryogenesis *and* have the LSP provide the full DM relic abundance, in part of the allowed parameter space. However, other possibilities for DM also exist, which are discussed. It is expected that upcoming direct DM searches as well as neutrino signals from DM annihilation in the Sun will be sensitive to this class of models. Interesting collider and Gravity-wave signals are also briefly discussed.

Contents

1	Introduction	1
2	Features of the Model	3
2.1	Theoretical Details	7
3	The $U(1)_R$ Symmetric Limit: $T = 0$ Analysis	9
4	A Strongly First-Order EWPT	13
5	Pseudo-Dirac Dark Matter - Constraints and Signals	20
5.1	Relic Abundance	21
5.2	Direct Detection	24
5.3	Indirect Detection	27
6	A Benchmark Example	29
7	\mathcal{CP} Phases - EWBG and EDM's	31
8	Other Experimental Signatures	34
8.1	Collider Signatures	35
8.2	Gravitational Waves	38
9	Summary and Conclusions	38
A	Expressions including R-breaking and $v_T \neq 0$	40
B	Approach IV: Details of the Model	43

1 Introduction

Although the Standard-Model is an excellent description of Nature up to energies of around a hundred GeV, it fails to explain two of the most important mysteries of our Universe - the nature of Dark Matter (DM) and the origin of the matter-antimatter asymmetry.¹ Many candidates for Dark Matter - axions, gravitinos, WIMPs, etc. exist; however the most popular among them is the WIMP, which can provide the observed relic abundance from a thermal freeze-out mechanism in a large region of parameter space. Moreover, such a particle also arises within

¹We have nothing to say in this paper about the *biggest* mystery - the tiny value of the Cosmological Constant.

many schemes of beyond-the-Standard-Model physics such as low-scale supersymmetry, extra dimensions, etc.

Similarly, many popular mechanisms for generating the matter-antimatter asymmetry exist. These can be broadly divided into those which depend on physics at very high scales and those which depend on physics at the electroweak (EW) scale and below. Models in the first class include models of GUT baryogenesis [1] and leptogenesis [2]. On the other hand models in the second class include those of electroweak baryogenesis [3], TeV-scale leptogenesis [4] and Affleck-Dine baryogenesis [5]. There also exist models which propose to explain both the baryon asymmetry of the universe (BAU) and the DM abundance as an *asymmetry* in a conserved charge [6]-[11], [12], although they typically involve a very weakly coupled “hidden” sector.

Electroweak baryogenesis is attractive since it only depends on physics in the visible sector at the electroweak scale; hence the mechanism is completely testable (at least in principle) at colliders probing energies of order the electroweak scale, or astrophysical/cosmological observations probing temperatures (or times) of order the electroweak scale. Supersymmetric extensions of the Standard Model provide an elegant solution to the hierarchy problem as well as a Dark Matter candidate in the form of the lightest supersymmetric particle or LSP (assuming R -parity conservation). However, within the minimal supersymmetric Standard Model (MSSM), the allowed region for a strongly first-order phase transition, which is one of the important requirements for electroweak baryogenesis, is severely constrained [13] and will soon be tested by experiments (see [14] for a recent review). In addition, there is tension between having enough CP violation to produce the required baryon asymmetry and constraints from electric dipole-moment (EDM) searches [15]. It is, therefore, worthwhile to study extensions of the MSSM with additional terms in the tree-level scalar potential which could help in making the transition strongly first-order.² The viability of singlet extensions of the MSSM with regard to electroweak baryogenesis has been widely studied [18] [19]. In particular, Ref. [19] studied a singlet extension of the MSSM called the nMSSM, in which it was shown that it was possible to have a strongly first-order phase transition as well as generate the correct relic abundance for the lightest neutralino. The lightest neutralino in that case is, however, not completely stable but has a lifetime longer than the age of the Universe.

In this work, we explore a different extension of the MSSM which can give rise to electroweak baryogenesis and a WIMP DM candidate. Assuming standard cosmology, the freeze-out abundance of the WIMP can account for the full DM abundance in part of the allowed parameter space. It is also possible for the WIMP to form an $\mathcal{O}(1)$ fraction of the DM, or a negligible frac-

²Alternatively, it has been argued that new fermions, strongly coupled to the SM, can also strengthen the EWPT, and lead to a EWBG/DM connection [16]. Ideas for generating the baryon asymmetry at the TeV scale *without* a strongly first-order EWPT have also been proposed [17].

tion of DM, in other regions of the allowed parameter space. The WIMP DM candidate in the framework is completely stable. In addition, the tension with EDM searches is largely relaxed or inexistent. A crucial feature of the model is the existence of an (approximate) $U(1)_R$ -symmetry, leading to the following important consequences:

- The R -symmetry leads to new interactions in the scalar potential which help make the phase transition strongly first-order.
- Since global symmetries are expected to be violated by gravitational effects, “small” R -breaking effects are included. The R -symmetry can thus be thought of as an accidental symmetry of the low-energy theory. As we will see, the small R -breaking helps in achieving many phenomenologically desirable features at the same time:
 - a) *Viable down-type fermion masses in some realizations (others do not require R -breaking).*
 - b) *Evade stringent direct-detection bounds from XENON100.*
 - c) *Obtain a relic abundance consistent with observations in part of parameter space.*
- The CP-violation required for baryogenesis may have two origins: a) There are explicit CP phases in the parameters of the scalar potential, resulting in complex, spacetime-dependent v_{ev} s, inducing CP-violating phases in the mass matrices for the charginos and neutralinos, or b) All parameters in the scalar potential are real and CP violation arises from the phases in the R -symmetry breaking Majorana masses of the charginos and neutralinos. In both cases, the approximate R -symmetry suppresses the contribution to EDMs relative to that in the non R -symmetric case.

The plan of the paper is as follows. In Section 2 we present the relevant features of the R -symmetric scenarios, and discuss a number of realizations and theoretical considerations. In Section 3, we discuss the zero-temperature properties of such models, while in Section 4 we analyze the finite-temperature potential and explain the origin of the strongly first-order phase transition. In Section 5, we discuss several aspects related to DM (relic density, direct and indirect searches), and its connection to the first-order electroweak phase transition (EWPT). In Section 7 we briefly comment on the generation of the baryon-asymmetry of the Universe (BAU), and discuss the reasons that allow to satisfy EDM constraints, even with sfermion masses at around a TeV. Finally, we consider other signatures in Section 8, and conclude in Section 9. We also include two appendices with technical details.

2 Features of the Model

In this section, we describe the structure of the model at the electroweak scale in detail. An R -symmetry is well motivated from a theoretical point of view. In the global limit, having an

exact R -symmetry allows one to construct simple models of dynamical supersymmetry breaking in accord with the Nelson-Seiberg theorem [20]. A unique anomaly-free R -symmetry also arises in a superconformal field theory at the superconformal fixed point, which can be found by a -maximization [21]. One of the first phenomenological models with R -symmetry was written down in [22].

Having an R -symmetry gives rise to many interesting phenomenological features. For example, Majorana gaugino masses, trilinear A parameters, and the $B\mu$ parameter are forbidden. However, gaugino masses of the Dirac type are allowed.³ As a result, this leads to a significant suppression of flavor and CP-violating effects relative to the MSSM for $\mathcal{O}(1)$ flavor-violating soft scalar masses and phases [24]. Although the minimal R -symmetric spectrum does not give rise to gauge coupling unification, many scenarios for adding additional matter have been proposed which could help unify the couplings [23, 25, 26, 27].

The minimal R -symmetric spectrum is shown in Table 1 with the possible R -charge assignments. The origin of these assignments can be understood as follows. The R -charges of the adjoints $\{S, T, O\}$ are chosen to ensure that a Dirac gaugino mass term can be written down with a D SUSY-breaking spurion. The simplest R -charge assignment of the Q, U^c , and H_u superfields, so that the up-type Yukawa couplings are allowed, is given by⁴ $R[Q, U^c] = 1, R[H_u] = 0$. This leaves the R -charges of the D^c, E^c, L and H_d superfields. A number of approaches can be followed about the R -charges of these fields and the associated couplings:

- I. One approach to down-type fermion masses was taken in [27] with $R[H_d] = 2, R[D^c, E^c] = -1$, and $R[L] = 1$. This allows down-type Yukawa couplings in the superpotential, at the expense of making the R -symmetry anomalous with respect to $SU(3)_C$. However, since the R symmetry is best thought of as an accidental symmetry, this does not appear to be an issue. There are two ways of generating viable down-type fermion masses in this scheme. Small R -breaking effects could arise from Majorana gaugino masses and/or A parameters, which could generate down-type fermion masses at 1-loop [29]. Alternatively, R -breaking could arise from a $B\mu$ term, leading to a small vev for H_d and providing viable down-type fermion masses via the usual holomorphic Yukawa couplings.
- II. A model with $R[L, D^c, E^c] = 1$ and $R[H_d] = 2$ is considered in [28], which makes the R -symmetry anomaly free. In this case, down-type Yukawa couplings are forbidden in the superpotential, but down-type fermion masses can still be generated by supersymmetry-breaking terms in the Kähler potential. Generating viable fermion masses and an electroweak scale μ -term then implies that the supersymmetry breaking scale is quite low.

³Dirac gaugino masses can also be motivated from “supersoft” supersymmetry breaking in which the gauge sector has $\mathcal{N} = 2$ supersymmetry [23].

⁴These terms must be allowed without suppression since the top mass arises from these.

Superfield	$3 \times 2 \times 1$	$U(1)_R$			
Q	$(\mathbf{3}, \mathbf{2})_{1/6}$	1	1	1	1
U^c	$(\bar{\mathbf{3}}, \mathbf{1})_{-2/3}$	1	1	1	1
D^c	$(\bar{\mathbf{3}}, \mathbf{1})_{1/3}$	-1	1	1	1
L	$(\mathbf{1}, \mathbf{2})_{-1/2}$	1	1	1	1
E^c	$(\mathbf{1}, \mathbf{1})_1$	-1	1	1	1
H_u	$(\mathbf{1}, \mathbf{2})_{1/2}$	0	0	0	0
H_d	$(\mathbf{1}, \mathbf{2})_{-1/2}$	2	2	0	2
S	$(\mathbf{1}, \mathbf{1})_0$	0	0	0	0
T	$(\mathbf{1}, \mathbf{3})_0$	0	0	0	0
O	$(\mathbf{8}, \mathbf{1})_0$	0	0	0	0
R_u	$(\mathbf{1}, \mathbf{2})_{-1/2}$	-	-	2	-
R_d	$(\mathbf{1}, \mathbf{2})_{+1/2}$	-	-	2	-
H'_u	$(\mathbf{1}, \mathbf{2})_{+1/2}$	-	-	-	2
H'_d	$(\mathbf{1}, \mathbf{2})_{-1/2}$	-	-	-	0

Table 1: Quantum numbers of the superfields in the model. The four entries for the R -charges of the superfields D^c , E^c , H_d correspond to their values in approaches I-IV described in the main text. The fields $\{R_u, R_d\}$ and $\{H'_u, H'_d\}$ only exist in approaches III and IV, respectively.

Also, [28] considered a version of the model without the singlet S .

- III. Both up-type and down-type fermion masses are allowed if $R[H_d] = 0$, and $R[L, D^c, E^c] = 1$. However, terms like $\mu H_u H_d$ and $\lambda_s S H_u H_d$ which generate Higgsino masses are forbidden. Viable Higgsino masses can however be generated by having additional vector-like doublets R_u and R_d with R -charges $R[R_u, R_d] = 2$, which also makes the R -symmetry anomaly free [24, 30].

How does our approach compare with those above? The two main issues of interest in this paper are the existence of a strongly first-order electroweak phase transition (EWPT), and of a WIMP DM candidate which could provide all or some of the DM relic abundance and have a signal in DM experiments. It turns out that within the R -symmetric setup, the former can be naturally achieved in the presence of the superpotential term $\lambda_s S H_u H_d$ and the *potential* term $t_s S + h.c.$ (as discussed in Section 3). This implies that $R[H_d] = 2$. The requirement of a strongly first-order EWPT, therefore, seems to suggest that we either follow approach I, or approach II (with the singlet field taken into account). However, even with the singlet, approach II requires very low-scale supersymmetry breaking which typically gives rise to an extremely light non-WIMP gravitino DM candidate –not desirable from our point of view. Approach III does not work within our framework since it assumes $R[H_d] = 0$.

However, it is possible to use an approach which is a combination of that in II and III, and

is consistent with our requirements. We call it approach IV and briefly describe it below (we give further details in Appendix B).

- IV. We use the same set of fields as in approach III but focus on a different region of parameter space. An appropriate redefinition of the fields H_d , R_u and R_d in approach III can give rise to viable down-type fermion masses while keeping the R -symmetry intact. The R -charges of L, D^c, E^c are equal to unity, the same as in approach II and III. However, we redefine the three fields H_d , R_u , and R_d with $R[H_d] = 0$, $R[R_u] = 2$, $R[R_d] = 2$ in approach III in the following way:

$$\{H_d, R_u, R_d\} \rightarrow \{H'_d, H_d, H'_u\} , \quad (1)$$

respectively, so that $R[H_d] = 2$, $R[H'_u] = 2$, $R[H'_d] = 0$. Since $R[H_d] = 2$ now, the coupling $\lambda_s S H_u H_d$ is allowed and a strongly first order EWPT is possible. Furthermore, down-type fermion masses are generated from supersymmetry breaking similar to that in approach II but with an important difference. The down-type fermion masses are only suppressed by the masses of H'_u and H'_d , not the messenger mass M_\star as in approach II. Hence, viable down-type fermion masses *without* R -symmetry breaking can be generated for high supersymmetry breaking scales as long as $M_{H'_u}$ and $M_{H'_d}$ are only slightly above the superpartner mass scale. When the R -symmetry is ultimately broken by gravitational effects leading to a tiny vev for H_d , there will be an additional contribution to down-type masses, which will generically be quite suppressed compared to the one above.

Thus, both approach I and IV are consistent with the framework considered in this paper, and we will consider both possibilities. We will show, however, in section 7 that the two approaches can in principle lead to different predictions for EDMs. Finally, let us comment on the μ -term, which is allowed by the R -charges. Here we assume that a large μ -term (compared to the EW scale) is absent in the microscopic theory which gives rise to the R -symmetric theory at the electroweak scale. For example, string selection rules often exponentially suppress coefficients of terms in the superpotential which are otherwise allowed by low energy effective field theory [31]. Thus, it is possible to naturally have an EW scale μ term.⁵ It is then possible to absorb an EW scale μ parameter by a redefinition of S . Although the μ -term appears in the parameters of the scalar potential, since we will consider the most general form of the potential consistent with the R symmetry, and with all mass parameters of order the electroweak scale, there is no loss of generality.

⁵Any value of μ is *technically* natural.

2.1 Theoretical Details

We envision the following simple model of supersymmetry breaking which preserves an approximate $U(1)_R$, as already discussed in [30]. We will, therefore, be brief and only highlight the main features. We assume a hidden supersymmetry breaking sector with gauge interactions including a $U(1)$ gauge field \mathcal{W}'_α which gets a nonvanishing D -term, and chiral superfields X charged under the hidden sector gauge group which get non-vanishing F -terms. X and \mathcal{W}'_α are assumed to have R -charges 2 and 1, respectively. Supersymmetry breaking is then mediated to the visible sector by interactions suppressed by the mediator mass M_\star . Since we want to be as model-independent as possible, we will leave this mass scale unspecified. Although in this work we will not be concerned with embedding the model at the electroweak scale in a UV complete microscopic theory, it is not hard to envision a variety of ways, which may or may not require a very small value of \sqrt{F} ,⁶ in which this can be done. Requiring a WIMP DM candidate, however, implies that the supersymmetry breaking scale be large. Note that this does *not* automatically imply gravity or anomaly mediated supersymmetry breaking, as high-scale gauge mediation models with neutralino LSP can be constructed [32].

With the above considerations in mind, in addition to the kinetic terms, the Lagrangian of our model is given by:

$$L = L_W + L_{\text{down}} + L_{\text{soft}} , \quad (2)$$

$$L_W = \int d^2\theta (\mathbf{y}_u Q U^c H_u + \lambda_s S H_u H_d + \lambda_T T H_u H_d) + \text{h.c.} , \quad (3)$$

$$L_{\text{down}} = \int d^2\theta (\mathbf{y}_d Q D^c H_d + \mathbf{y}_e L E^c H_d) + \text{h.c.} , \quad \text{or} \quad (4)$$

$$\int d^4\theta \left(\mathbf{y}_d \frac{\mathcal{D}^\alpha Q \mathcal{D}_\alpha D^c H_u^\dagger}{M_{H'_d}^2} \frac{X^\dagger X}{M_\star^2} + \mathbf{y}_e \frac{\mathcal{D}^\alpha L \mathcal{D}_\alpha E^c H_u^\dagger}{M_{H'_d}^2} \frac{X^\dagger X}{M_\star^2} \right) + \text{h.c.} ,$$

$$L_{\text{soft}} = \sqrt{2} c_a \int d^2\theta \left(\frac{\mathcal{W}'^\alpha}{M_\star} \right) \mathcal{W}'_\alpha \Sigma_a + \text{h.c.} + \quad (5)$$

$$\left[c_a^D \int d^2\theta \left(\frac{\mathcal{W}'^\alpha \mathcal{W}'_\alpha}{M_\star^2} \right) \Sigma_a^2 + \text{h.c.} \right] + c_a^F \int d^4\theta \left(\frac{X^\dagger X}{M_\star^2} \right) (\Sigma_a^2 + \text{h.c.}) + \quad (6)$$

$$c_{ij}^F \int d^4\theta \left(\frac{X^\dagger X}{M_\star^2} \right) Q_i^\dagger Q_j , \quad (7)$$

where $a = U(1)_Y, SU(2)_L, SU(3)_C, \Sigma_a \equiv \{S, T, O\}$, and Q_i runs over all matter fields. Note that since there are no gauge singlets with supersymmetry breaking F -terms, the standard trilinear parameters and the $B\mu$ parameter vanish. Let us now comment on the operators above.

⁶Still with superpartner masses around the electroweak scale.

The operators in L_W include the holomorphic Yukawa couplings for the up-quark sector. Operators in L_{down} are responsible for down-type fermion masses. These can either arise from holomorphic Yukawa couplings (as in approach I) or by supersymmetry breaking (as in approach IV described above and in Appendix B). The qualitative details of our analysis for the nature of the phase transition and WIMP DM abundance are essentially *independent* of the two approaches, hence the results obtained here apply equally well to both approaches.

Operator (5) in L_{soft} not only gives rise to Dirac gaugino masses, $M_{D_a} \equiv c_a \frac{\langle D \rangle}{M_\star}$, but also to mass terms for the real part of the adjoint scalars $\text{Re}(\Sigma_a)$ as well as “trilinear” couplings of the form $(M_a \Sigma_a + \text{h.c.}) (g_a \sum_i \tilde{q}_i^* \mathbf{T}^a \tilde{q}_i)$ [23]. These new trilinear couplings will be relevant when we discuss the EWPT in Section 3. Operator (6) can be written for fields in real representations of the gauge group, hence it provides (equal and opposite) mass-squared terms for the real and imaginary parts of Σ_a . Operator (7) generates the standard soft mass-squareds for all scalars. Note that the adjoint scalars Σ_a receive masses from all three operators above, resulting in different masses for their real and imaginary parts.

Since the hypercharge adjoint is a singlet S with vanishing R -charge, it is possible to write a trilinear parameter for it:

$$c_s \int d^4\theta \left(\frac{X^\dagger X}{M_\star^3} \right) S^3 + \left[c'_s \int d^2\theta \left(\frac{\mathcal{W}'_\alpha \mathcal{W}'_\alpha}{M_\star^3} \right) S^3 + \text{h.c.} \right], \quad (8)$$

which is, however, parametrically suppressed relative to other parameters –it is of $\mathcal{O}(M_{\text{soft}}^2/M_\star)$ compared to $\mathcal{O}(M_{\text{soft}})$ for others. In general, there could be an anomaly-mediated contribution, which is also small compared to other soft terms. Higher powers of S appearing in the scalar potential will be suppressed even further. So we will neglect the above term (and other higher order powers of S) in our subsequent analysis.

As explained earlier, a small vev for H_d is induced once a $B\mu$ term is generated. Thus, it is natural to have $v_d \ll v_u$ in this framework. However, the precise value of the suppression depends on the mechanism of R -breaking. Note that the usual definition of “ $\tan \beta$ ” is not very appropriate, and will be discussed in Section 7. It is also important to clarify that there is no light (pseudo) scalar, like the R -axion. This is because the R -symmetry is broken explicitly by small amounts, *and* the same interactions which break the R -symmetry (such as the $B\mu$ term) generate a small vev for the R -charged H_d . Hence, the situation is similar to the MSSM with large $\tan \beta$ and small $B\mu$, in which there is no light pseudo-scalar. Finally, note that even in the presence of R -symmetry breaking by Majorana gaugino masses or the $B\mu$ term, a discrete Z_2 symmetry (call it R -parity) is preserved making the LSP completely stable.

As has been realized, there also exist potentially dangerous operators which must be sup-

pressed. These include:

$$\int d^2\theta \mathcal{W}'^\alpha \mathcal{W}_{\alpha Y} + \text{h.c.} , \quad (9)$$

$$\int d^2\theta \mathcal{W}'^\alpha \mathcal{W}'_\alpha S + \text{h.c.} , \quad \int d^4\theta \frac{X^\dagger X}{M_\star} S . \quad (10)$$

Operator (9) induces kinetic mixing between hypercharge and the hidden $U(1)$, and gives rise to an undesirable large hypercharge D -term, while operators (10) give rise to tadpole terms for the singlet S which could destabilize the electroweak hierarchy [33]. Suppressing the coefficients of operators arising from the superpotential is technically natural. Appealing to that is not possible for the coefficient of the operator coming from the Kähler potential, however.

Many possible mechanisms have been discussed in order to suppress the coefficients of the above operators. For example, in gravity-mediated models or higher-dimensional constructions this may happen if S originates from a non-abelian gauge theory (in many cases a GUT multiplet) which is unbroken at a scale not far from the TeV scale [30, 34]. Within gauge-mediation models, it is possible to avoid a large tadpole term if the couplings between adjoints and messengers respect a GUT symmetry [26], or if there is an appropriate parity symmetry forbidding a large tadpole term [35]. Finally, a large tadpole can be avoided if the theory itself has a low cutoff Λ_\star , close to the TeV scale [24]. Since the focus of the paper is not on detailed model-building, we will be agnostic about the precise embedding of the model in a UV complete theory and analyze the effective theory defined by (3)-(7), assuming that the operators in (9)-(10) are sufficiently suppressed, such that the singlet tadpole is of EW size. This will be crucial for the phase transition, as will be seen below.

3 The $U(1)_R$ Symmetric Limit: $T = 0$ Analysis

We are now in a position to study the scalar potential of the model. With the Lagrangian given in Eq. (2) of Section 2.1, the scalar potential takes the form:

$$V = V_F + V_D + V_{\text{soft}} + V_{\text{loop}}^{(1)} , \quad (11)$$

where

$$V_F = \sum_i \left| \frac{\partial W}{\partial \phi_i} \right|^2 , \quad V_D = \frac{1}{2} \sum_{a=1}^3 (D_2^a)^2 + \frac{1}{2} D_Y^2 , \quad (12)$$

$$V_{\text{soft}} = m_{H_u}^2 |H_u|^2 + m_{H_d}^2 |H_d|^2 + m_s^2 |S|^2 + m_T^2 T^{a\dagger} T^a \\ + B_T T^a T^a + t_s S + B_s S^2 + A_s S^3 + \text{h.c.} , \quad (13)$$

while $V_{\text{loop}}^{(1)}$ refers to the 1-loop contribution to the effective potential, which will be specified below. Here i runs over all fields appearing in the $U(1)_R$ -symmetric supersymmetric Standard Model, and D_Y and D_2^a are the hypercharge and $SU(2)_L$ D -terms, respectively. Compared to the MSSM case, the D -terms contain additional pieces associated with the $SU(2)_L$ and $U(1)_Y$ adjoint fields:

$$\begin{aligned} D_2^a &= g(H_u^\dagger \tau^a H_u + H_d^\dagger \tau^a H_d + T^\dagger \lambda^a T) + \sqrt{2}(M_{D_2} T^a + \text{h.c.}) , \\ D_Y &= g'(H_u^\dagger H_u - H_d^\dagger H_d) + \sqrt{2}(M_{D_1} S + \text{h.c.}) , \end{aligned} \quad (14)$$

where τ^a and λ^a are the two and three-dimensional $SU(2)$ generators respectively. Note that, as explained in Section 2.1, the D terms above give rise to new *trilinear* couplings in the scalar potential, which will be relevant when we discuss the phase transition. Also, the masses of the real and imaginary parts of $S = S_R + i S_I$ and $T = T_R + i T_I$ are split in Eq. (11). For instance, if M_{D_i} , B_s and B_T are real, then $m_{S_R}^2 = m_s^2 + 2B_s + 4M_{D_1}^2$, $m_{S_I}^2 = m_s^2 - 2B_s$, $m_{T_R}^2 = m_T^2 + 2B_T + 4M_{D_2}^2$ and $m_{T_I}^2 = m_T^2 - 2B_T$. In this section and the following we will assume that there are no CP-violating phases in the Higgs scalar potential. We will comment on the possible presence of such phases, and their connection to EWBG, in Section 7. Note also that, within approach IV, there exist additional fields H'_u and H'_d , but since they are assumed to be parametrically heavier than the other fields (see Appendix B), their effect on the minimization of the potential can be neglected .

In order to minimize the above potential, we point out two important simplifications. First, EW precision constraints require the triplet Higgs vev , $T^3 \equiv v_T$, to be small, which can be achieved if the triplet soft breaking mass, m_T^2 , is in the multi-TeV range. Therefore, the effect of the triplet on the minimization of the potential must be small, and we will set $v_T = 0$.⁷ In addition, we will analyze the potential in the R -symmetric limit. The $U(1)_R$ symmetry with our R -charge assignments implies that $b \equiv B\mu = 0$. Hence, if $m_{H_d}^2 > 0$, one can easily see that $\langle H_d \rangle = 0$ (i.e. we avoid spontaneous breaking of the $U(1)_R$ symmetry), and the degrees of freedom in H_d effectively decouple from the minimization of the potential. Therefore, the EW symmetry is broken by $\langle H_u^0 \rangle = v$, with $v \approx 174$ GeV, and the eaten Nambu-Goldstone bosons, as well as the SM-like Higgs, all arise from H_u . In particular, the vacuum is automatically charge-preserving, exactly as in the SM. Note that when R -symmetry is broken, there will be other terms in the scalar potential. However, those terms represent a small perturbation on the analysis based on the previous approximations, and do not affect the qualitative results.

The zero-temperature 1-loop contribution to the effective potential, in the R -symmetric

⁷We could keep track of the small triplet vev , but setting it to zero will make the physics more transparent.

limit,⁸ is given by $V_{\text{loop}}^{(1)} = \frac{1}{2} \Delta\lambda |H_u|^4$, where [37, 38]

$$\Delta\lambda \approx \frac{3y_t^2}{8\pi^2} \log\left(\frac{M_{\text{SUSY}}^2}{m_t^2}\right) \left[y_t^2 - \frac{1}{4}(g^2 + g'^2) \right], \quad (15)$$

with y_t the top Yukawa coupling and $m_t \approx 173$ GeV the top quark mass. Note that we do not write contributions to $\Delta\lambda$ from the A -terms, since these are forbidden by the $U(1)_R$ symmetry, and remain small provided the $U(1)_R$ violation is small. Thus, the size of $\Delta\lambda$ is controlled by M_{SUSY} , which can be taken as the geometric mean of the LH and RH stop masses.

Minimizing with respect to H_u^0 , we get the condition

$$\delta \equiv m_{H_u}^2 + \frac{1}{4}(g^2 + g'^2 + 4\Delta\lambda)v^2 + \sqrt{2}g'M_{D_1}v_s + \lambda_s^2v_s^2 = 0, \quad (16)$$

where v_s is the vev of S . We will also take advantage of the fact that A_s is expected to be parametrically suppressed with respect to the other parameters. So, neglecting A_s one gets the following relatively simple expression for v_s :

$$v_s = -\frac{2t_s + \sqrt{2}g'M_{D_1}v^2}{2(m_{S_R}^2 + \lambda_s^2v^2)}. \quad (17)$$

The vacuum in the above limit thus only depends on λ_s , $m_{S_R}^2$, t_s and M_{D_1} .

The spectrum of Higgses is as follows. Due to the constraints from EW precision measurements, the heaviest of the Higgs states are expected to be the excitations of the triplet T^a , with a mass of order $m_T \sim$ few TeV. There is also another charged Higgs and a *complex* neutral scalar, both arising from H_d , with masses

$$m_{H_d^0}^2 = m_{H_d}^2 + \left[\lambda_s^2 + \lambda_T^2 - \frac{1}{4}(g^2 + g'^2) \right] v^2 - \sqrt{2}g'M_{D_1}v_s + \lambda_s^2v_s^2, \quad (18)$$

$$m_{H_d^\pm}^2 = m_{H_d^0}^2 + \left(\frac{1}{2}g^2 - \lambda_s^2 - \lambda_T^2 \right) v^2, \quad (19)$$

which could also be somewhat heavy, depending on the soft mass $m_{H_d}^2$.

Finally, there is a CP-odd (singlet) scalar with mass $m_a^2 = m_{S_I}^2 + \lambda_s^2v^2 - 6A_s v_s$, as well as a pair of CP-even Higgs states that can have couplings to gauge boson pairs. The latter are linear superpositions of $h_u^0 = \text{Re}(H_u^0) - v$ and $s = S_R - v_s$, and the corresponding mass matrix in the $\{h_u^0, s\}$ basis reads:

$$\mathcal{M}_H^2 = \begin{pmatrix} \frac{1}{2}(g^2 + g'^2 + 4\Delta\lambda)v^2 + \delta & v[\sqrt{2}g'M_{D_1} + 2\lambda_s^2v_s] \\ v[\sqrt{2}g'M_{D_1} + 2\lambda_s^2v_s] & m_{S_R}^2 + \lambda_s^2v^2 + 6A_s v_s \end{pmatrix}, \quad (20)$$

⁸In approach IV of Section 2, where the $QD^c H_d$ superpotential term is forbidden, there are no terms in the one-loop effective potential involving H_d . In approach I, such terms are generated, but since we will always be in a situation where H_d is very small, these terms play only a minor role in the minimization of the potential.

where we included the dependence on A_s for completeness, although we expect it to be negligible. We also included in the (1, 1) entry the contribution from δ in Eq. (16): although it vanishes in the zero-temperature vacuum, it will give a non-vanishing contribution at finite temperature, when v and v_s are not identified with their zero-temperature values, and should be included in the analysis of the next section. Note that the CP-even states in (20) depend on the same set of microscopic parameters that determine the vacuum, while the remaining Higgses depend on additional parameters that do not affect the vacuum (in the limit defined above). Thus, the stability along the excitations of Eqs. (18) and (19), as well as the CP-odd singlet and the triplet directions, is easily guaranteed by the choice of $m_{H_d}^2$, $m_{S_I}^2$ and m_T^2 , respectively.

The neutralinos and charginos also play an important role in the collider phenomenology, the DM question, and the EWPT. Since the neutralinos are Dirac in nature in the R -symmetric limit, the mass matrix in the basis $\{i\tilde{B}, i\tilde{W}^0, \tilde{H}_d^0; \tilde{T}, \tilde{S}, \tilde{H}_u^0\}$ takes the form:

$$\mathcal{M}_{\chi^0} = \begin{pmatrix} 0 & \mathbf{X}_N \\ \mathbf{X}_N^T & 0 \end{pmatrix},$$

where

$$\mathbf{X}_N = \begin{pmatrix} 0 & M_{D_1} & m_Z s_w \\ M_{D_2} & 0 & -m_Z c_w \\ \lambda_T v & \lambda_s v & \lambda_s v_s \end{pmatrix}, \quad (21)$$

and we again set the triplet vev to zero.

Similarly, for the charginos we have in the $\{\tilde{T}^-, i\tilde{W}^-, \tilde{H}_d^-; \tilde{T}^+, i\tilde{W}^+, \tilde{H}_u^+\}$ basis:

$$\mathcal{M}_{\chi^\pm} = \begin{pmatrix} 0 & \mathbf{X}_C \\ \mathbf{X}_C^T & 0 \end{pmatrix},$$

where

$$\mathbf{X}_C = \begin{pmatrix} 0 & M_{D_2} & 0 \\ M_{D_2} & 0 & \sqrt{2} m_W \\ \sqrt{2} \lambda_T v & 0 & -\lambda_s v_s \end{pmatrix}. \quad (22)$$

At zero-temperature v_s is given by Eq. (17). Note that the neutralino and chargino mass matrices depend on two parameters that do not enter in the determination of the vacuum: λ_T and M_{D_2} . Furthermore, it is easy to find that the three chargino mass eigenvalues are given by

$$m_{\chi_1^\pm} = M_{D_2},$$

$$m_{\chi_{2,3}^\pm}^2 = \frac{1}{2} \left\{ M_{D_2}^2 + (g^2 + 2\lambda_T^2)v^2 + \lambda_s^2 v_s^2 \right. \quad (23)$$

$$\left. \pm \sqrt{[M_{D_2}^2 + (g^2 + 2\lambda_T^2)v^2 + \lambda_s^2 v_s^2]^2 - 4(\lambda_s M_{D_2} v_s + \sqrt{2} g \lambda_T v^2)^2} \right\}. \quad (24)$$

We see from the first equation that we must require $M_{D_2} \gtrsim 104$ GeV to avoid a chargino lighter than the direct LEP chargino bound [39]. However, we also note that we cannot take M_{D_2} arbitrarily large, since in that limit one finds $m_{\chi_{2\pm}} \approx \lambda_s v_s [1 + \mathcal{O}(v/M_{D_1}, v_s/M_{D_1})]$, which is typically smaller than the chargino LEP bound. Thus, the chargino bound selects a region in M_{D_2} which, together with the region in M_{D_1} and λ_s preferred by the minimization of the potential (and the requirement of a strongly first-order phase transition to be discussed in the next section) leads to a particular composition for the lightest neutralino, from Eq. (21). In particular, one finds a sizable Higgsino component, which has interesting consequences for the computation of the DM relic density and for direct DM searches, to be described in Section 5.

4 A Strongly First-Order EWPT

We now turn to the finite-temperature potential, focusing in particular on highlighting the reasons that lead to a strongly first-order electroweak phase transition (EWPT). We assume for concreteness that the early Universe had a high-enough temperature. The temperature decreases with the expansion of the Universe, and EWPT takes place at temperatures of $\mathcal{O}(T_{EW}) = M_{EW}$, which is the object of our study in the following. The main effects arise already at “tree-level”, so that it will be sufficient to simply consider the thermal masses induced by the plasma. A more refined analysis based on the full finite-temperature effective potential is possible, but is not expected to change the conclusions other than in small details. This is to be contrasted with the case of the MSSM (or the SM), where carefully considering up to two-loop (“daisy” improved) effects [40] is essential to determine the strength of the phase transition (see [14] for a recent review).

We continue –as in the previous section– to consider the limit where the triplet Higgses are heavy so that the triplet vev is sufficiently suppressed to be consistent with the constraints on the Peskin-Takeuchi T -parameter. Therefore, these particles are effectively decoupled from the plasma. However, we will assume that the four real degrees of freedom in H_d and the CP-odd singlet scalar S_I can be considered as light degrees of freedom at the temperatures of interest (all the masses below $\sim \pi T_c$, where T_c is the critical temperature). The two CP-even Higgs states from the h_u^0 - s system, and the neutralinos/charginos are also light, hence active in the plasma during the EWPT.

In the $U(1)_R$ symmetric limit considered in the previous section, the minimization of the potential at finite temperature effectively involves only two degrees of freedom: $\phi \equiv H_u^0$ and the singlet scalar, $\phi_s \equiv S_R$ (at zero temperature, $\langle \phi \rangle = v$ and $\langle \phi_s \rangle = v_s$). The thermal masses can be read directly from the terms involving $\langle H_u^0 \rangle = v$ and $\langle S_R \rangle = v_s$ given in the previous section. We use the high-temperature expansion for the effective potential, so that the leading

T -dependent terms are obtained from

$$\begin{aligned}
V_T(\phi, \phi_s) &= \frac{1}{24} T^2 \left[2m_{H_d^0}^2 + 2m_{H_d^\pm}^2 + m_a^2 + \text{Tr} \mathcal{M}_H^2 + 6m_W^2 + 3m_Z^2 \right] \\
&\quad + \frac{1}{48} T^2 \left[2 \text{Tr}(\mathcal{M}_{\chi^0}^\dagger \mathcal{M}_{\chi^0}) + 2 \text{Tr}(\mathcal{M}_{\chi^\pm}^\dagger \mathcal{M}_{\chi^\pm}) + 12m_t^2 \right] \\
&\equiv c_\phi T^2 \phi^2 + c_{S^2} T^2 \phi_s^2 + c_S T^2 \phi_s + \text{const.} , \tag{25}
\end{aligned}$$

where we can drop the field-independent constants, and

$$c_\phi = \frac{11}{32} g^2 + \frac{3}{32} g'^2 + \frac{1}{4} y_t^2 + \frac{1}{8} \Delta\lambda + \frac{1}{4} \lambda_s^2 + \frac{1}{3} \lambda_T^2 , \tag{26}$$

$$c_{S^2} = \frac{3}{8} \lambda_s^2 , \quad c_S = -\frac{1}{4\sqrt{2}} g' M_{D_1} . \tag{27}$$

We also included the contributions from the electroweak gauge bosons and the top quark: $m_W^2 = \frac{1}{2} g^2 \phi^2$, $m_Z^2 = \frac{1}{2} (g^2 + g'^2) \phi^2$ and $m_t = y_t \phi$ (in the $\tan\beta = \infty$ limit). The finite-temperature potential then takes the form

$$V = (\tilde{m}^2 \phi^2 + \tilde{\lambda} \phi^4) + (2\tilde{t}_s \phi_s + \tilde{m}_s^2 \phi_s^2 + A_s \phi_s^3) + (2\tilde{a}_s \phi_s \phi^2 + \tilde{\lambda}_s \phi_s^2 \phi^2) , \tag{28}$$

where the effective coefficients (denoted by a tilde) are given in terms of the parameters of Eqs. (11) and (26)-(27) by

$$\begin{aligned}
\tilde{m}^2 &= m_{H_u}^2 + c_\phi T^2 , & \tilde{a}_s &= \frac{1}{\sqrt{2}} g' M_{D_1} , & \tilde{\lambda} &= \frac{1}{8} (g^2 + g'^2) + \frac{1}{2} \Delta\lambda , \\
\tilde{m}_s^2 &= m_{S_R}^2 + c_{S^2} T^2 , & \tilde{t}_s &= t_s + \frac{1}{2} c_S T^2 , & \tilde{\lambda}_s &= \lambda_s^2 .
\end{aligned} \tag{29}$$

The potential of Eq. (28) captures the physics to a good approximation even when allowing for a non-zero but small triplet vev , and for small $U(1)_R$ violating effects that can induce a small H_d vev .

We have split the terms in Eq. (28) into terms that depend only on ϕ , terms that depend only on ϕ_s , and terms that mix ϕ and ϕ_s . In order to understand the minimization of this system, and to highlight the underlying mechanism that leads to a strongly first-order phase transition, it is useful to start from the situation where the mixing terms vanish. In addition, we will make use of the fact that A_s is expected to be small [see comments following Eq. (8)], and we will neglect it in the following. Then one can see that the potential defines two scales: $-\tilde{m}^2/(2\tilde{\lambda})$ ($= \phi^2$ if $\tilde{m}^2 < 0$), and $\phi_s = -\tilde{t}_s/\tilde{m}_s^2$. We are interested in understanding the effects of a non-vanishing singlet vev on ϕ once the mixing terms are taken into account. This can be understood in a transparent way by writing an effective potential for ϕ after ‘‘integrating out’’ ϕ_s at tree-level (i.e. using the ϕ_s EOM). The mixing terms introduce a further scale into the

problem, $\phi_{\text{tr}}^2 \equiv \tilde{m}_s^2/\tilde{\lambda}_s$, that defines a transition field value for ϕ , below which the mixing terms are a small contribution to the potential compared to the pure singlet terms, and above which they dominate over the pure singlet terms. For instance, in the region where $\phi \ll \phi_{\text{tr}}$ one has

$$\phi_s = -\frac{\tilde{t}_s}{\tilde{m}_s^2} \left\{ 1 + \left(\frac{\tilde{a}_s \tilde{m}_s^2}{\tilde{\lambda}_s \tilde{t}_s} - 1 \right) \left[\frac{\phi^2}{\phi_{\text{tr}}^2} + \mathcal{O}\left(\frac{\phi^2}{\phi_{\text{tr}}^2}\right)^2 \right] \right\}, \quad (30)$$

and replacing back in Eq. (28) one finds the effective potential for ϕ :

$$V_{\text{eff}}(\phi) = -\frac{\tilde{t}_s^2}{\tilde{m}_s^2} + m_{\text{eff}}^2 \phi^2 + \lambda_{\text{eff}} \phi^4 + \mathcal{O}(\phi^6) \quad \text{for } \phi \ll \phi_{\text{tr}}, \quad (31)$$

where

$$m_{\text{eff}}^2 = \tilde{m}^2 - \frac{2\tilde{a}_s \tilde{t}_s}{\tilde{m}_s^2} + \frac{\tilde{\lambda}_s \tilde{t}_s^2}{\tilde{m}_s^4}, \quad (32)$$

$$\lambda_{\text{eff}} = \tilde{\lambda} - \frac{1}{\tilde{m}_s^6} \left[\tilde{\lambda}_s \tilde{t}_s - \tilde{a}_s \tilde{m}_s^2 \right]^2. \quad (33)$$

We see that one important effect of the singlet *vev* is that it gives a *negative* contribution to the effective quartic coupling near the origin. In fact, as we will see, the condition $\lambda_{\text{eff}} < 0$ characterizes the potentials that exhibit a (strongly) first-order phase transition at tree-level.⁹ The “instability” signaled by the negative effective quartic coupling indicates that there is a minimum far away from the origin. In the small field expansion of Eq. (31), this “far away” minimum can be understood as arising from balancing the quartic operator against the tower of higher-dimension operators in Eq. (31).

That the “far away” minimum exists in the above situation is guaranteed by the fact that (softly broken) supersymmetric potentials are bounded from below. One can see this explicitly by considering the case where $\phi \gg \phi_{\text{tr}}$. In this region, the mixing terms in Eq. (28) dominate over those that depend only on the singlet, and therefore the singlet *vev* is now given approximately by

$$\phi_s = -\frac{\tilde{a}_s}{\tilde{\lambda}_s} \left[1 + \mathcal{O}\left(\frac{\phi_{\text{tr}}^2}{\phi^2}\right) \right], \quad (34)$$

so that

$$V_{\text{eff}}(\phi) = \text{const.} + \left(\tilde{m}^2 - \frac{\tilde{a}_s}{\tilde{\lambda}_s} \right) \phi^2 + \tilde{\lambda} \phi^4 + \mathcal{O}(1/\phi^2), \quad \text{for } \phi \gg \phi_{\text{tr}}. \quad (35)$$

Thus, the original (positive) quartic operator controls the large-field behavior of the potential, while the singlet *vev* affects only the quadratic and other subdominant terms.

⁹This point has also been noted in [41].

The above arguments suggest that there is a first-order phase transition, and that it can easily be strong. Indeed, if $m_{\text{eff}}^2 > 0$ (either at $T = 0$ or due to the thermal mass contribution), then there is a local minimum at the origin, that can be separated by a barrier from the “far away” minimum described above. For this to be the case, one must also have that the effective mass, m_{eff}^2 , should not be excessively positive, or else it will overwhelm the effect of the negative quartic operator. On the other hand, if this squared mass is negative at $T = 0$, the thermal mass contribution will make it eventually positive, and there will exist a barrier provided only that $\lambda_{\text{eff}} < 0$. If the symmetry breaking minimum is the global minimum, then the main effect of increasing the temperature is to raise the global minimum to be degenerate with the minimum at the origin at some critical temperature T_c . It is worth emphasizing that this mechanism does not rely on the existence of a term cubic in ϕ , and is therefore qualitatively different from the way the phase transition works in the MSSM (or, had the Higgs been light enough, in the SM). As we will see, this allows more easily for the phase transition to be *strongly* first-order.

Potentials of the form of Eq. (28) were analyzed in Ref. [19], in the limit that the temperature dependence of \tilde{m}_s^2 and \tilde{t}_s is neglected, i.e. setting $\tilde{m}_s^2 = m_{S_R}^2$ and $\tilde{t}_s = t_s$ in Eq. (29). The model studied in that work was different from ours, and therefore the relation of the effective parameters to the underlying ones is different in the two cases. However, at the level of the effective parameters the two scenarios are identical, and we simply summarize the main results of the analysis in [19]. Defining the critical temperature T_c and the critical *vev* ϕ_c ($= \langle \phi \rangle$ at T_c) by:

$$V(\phi_c, T_c) = V(\phi = 0, T_c) , \quad (36)$$

$$\left. \frac{\partial V}{\partial \phi} \right|_{\phi=\phi_c} = 0 , \quad (37)$$

one finds

$$\phi_c^2 = \frac{1}{\tilde{\lambda}_s} \left(-m_{S_R}^2 + \frac{1}{\tilde{\lambda}} \left[m_{S_R} \tilde{a}_s - \frac{\tilde{\lambda}_s t_s}{m_{S_R}} \right] \right) , \quad (38)$$

$$T_c^2 = \frac{1}{c_\phi} [F(\phi_c^2) - F(v^2)] , \quad (39)$$

where c_ϕ was defined in Eq. (26), and

$$F(\phi^2) \equiv -2\tilde{a}_s \phi_s - \tilde{\lambda}_s \phi_s^2 - 2\tilde{\lambda} \phi^2 .$$

Here, it is understood that

$$\phi_s = -\frac{2t_s + \sqrt{2}g' M_{D_1} \phi^2}{2(m_{S_R}^2 + \lambda_s^2 \phi^2)} ,$$

which should be compared to Eq. (17). Based on the requirement that $\phi_c^2 > 0$, the authors of Ref. [19] derived a necessary condition for a first-order phase transition that can be seen to be equivalent to the requirement that $\lambda_{\text{eff}}(T=0) < 0$, where λ_{eff} is the effective quartic coupling in the small ϕ expansion, as defined in Eq. (33). Our previous comments then give a transparent interpretation for this condition in regards to the existence of a barrier separating a minimum at the origin from a “far away” minimum. Furthermore, it clarifies why this is only a necessary –but not a sufficient– condition for obtaining two degenerate minima separated by a barrier, and allows a generalization to the case that the temperature dependence in \tilde{m}_s^2 and \tilde{t}_s is included. As already mentioned, if the zero-temperature effective mass parameter, m_{eff}^2 is positive and excessively large, it may overwhelm the negative quartic operator in the small ϕ region. What is required is that there exist an “intermediate” region where the quartic operator can become relevant: at very small ϕ , the potential is determined by the quadratic term, while at large ϕ the higher-dimension operators [in the language of Eq. (31)] dominate. For instance, the coefficient of the ϕ^6 term in Eq. (31) is given by $G_{\text{eff}} \equiv \tilde{\lambda}_s(\tilde{a}_s\tilde{m}_s^2 - \tilde{\lambda}_s\tilde{t}_s)^2/\tilde{m}_s^8 > 0$. Thus, we see that the “far away” minimum is of order $\phi_c \sim \sqrt{-\lambda_{\text{eff}}/G_{\text{eff}}}$, which is obtained by balancing the ϕ^4 and ϕ^6 operators (the actual value of the “far away” v_{ev} depends on the full “tower of operators” in Eq. (31), but the above approximation captures the qualitative dependence up to an order one coefficient). Therefore, by requiring that the quadratic term not be larger than the quartic one for $\phi_c \sim \sqrt{-\lambda_{\text{eff}}/G_{\text{eff}}}$, one finds that one must also have $G_{\text{eff}}m_{\text{eff}}^2 \lesssim \lambda_{\text{eff}}^2$. Strictly speaking, the above relations ($\lambda_{\text{eff}} < 0$ and a not too large m_{eff}^2) should hold at the critical temperature, where the existence of the barrier is crucial. However, an approximate criterion for a first order phase transition in terms of microscopic parameters is

$$\begin{aligned} \lambda_{\text{eff}}|_{T=0} &= \tilde{\lambda} - \frac{1}{m_{S_R}^6} \left[\tilde{\lambda}_s t_s - \tilde{a}_s m_{S_R}^2 \right]^2 < 0, \\ G_{\text{eff}} m_{\text{eff}}^2|_{T=0} &= \frac{\tilde{\lambda}_s (\tilde{a}_s m_{S_R}^2 - \tilde{\lambda}_s t_s)^2}{m_{S_R}^8} \left[\tilde{m}^2 - \frac{2\tilde{a}_s t_s}{m_{S_R}^2} + \frac{\tilde{\lambda}_s t_s^2}{m_{S_R}^4} \right] \lesssim \lambda_{\text{eff}}^2|_{T=0}. \end{aligned} \quad (40)$$

Note that if $m_{\text{eff}}^2|_{T=0} < 0$, the second condition is automatic.

The condition that $T_c^2 > 0$ [as obtained from Eq. (39)] was also considered in Ref. [19]. This condition also has a simple interpretation: it is equivalent to requiring that the “far away” minimum be the global one (at $T=0$). The EW-preserving minimum has $\phi=0$ and $\phi_s = -t_s/m_{S_R}^2$, which leads to an associated potential energy $V_0 = -t_s^2/m_{S_R}^2$ [see Eq. (31)]. At the “far away” minimum one has

$$V(v, v_s) - V_0 = -\frac{v^4}{(1 + \tilde{\lambda}_s v^2/m_{S_R}^2)} \left\{ \lambda_{\text{eff}} + 2\tilde{\lambda}\tilde{\lambda}_s \left(1 + \frac{\tilde{\lambda}_s v^2}{2m_{S_R}^2} \right) \frac{v^2}{m_{S_R}^2} \right\}, \quad (41)$$

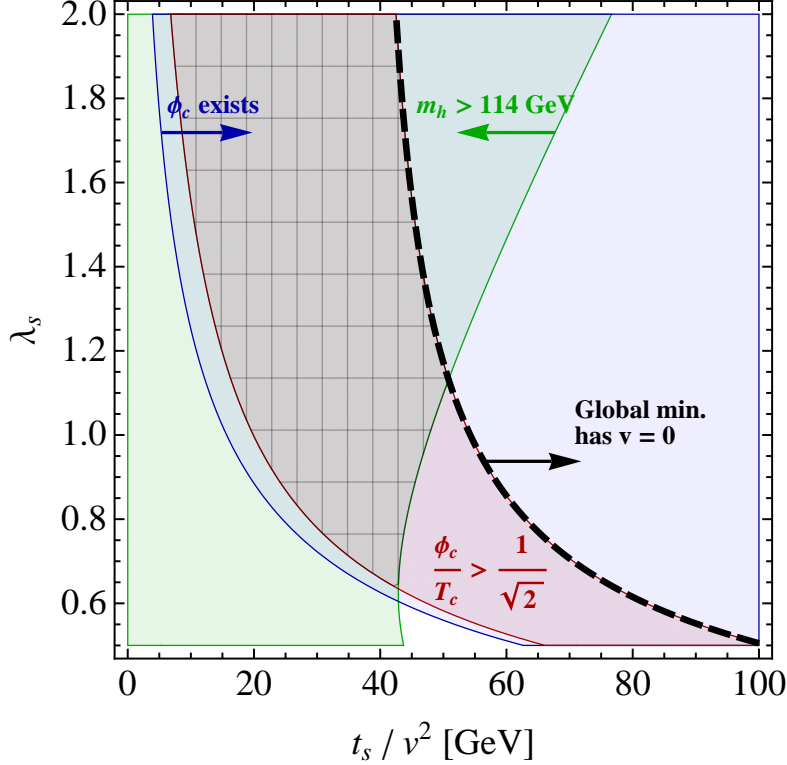


Figure 1: The hatched region in the t_s - λ_s plane leads to a strongly first-order phase transition (red) and is allowed by the Higgs LEP bound (green). We have fixed $M_{D_1} = 35$ GeV, $m_{S_R} = 100$ GeV and $M_{\text{SUSY}} = 2$ TeV.

where λ_{eff} , as given in Eq. (33), is evaluated at $T = 0$ and v_s is given in Eq. (17). Requiring that this expression be negative (to ensure that the EWSB minimum is the global one), results in the condition

$$\tilde{\lambda} < \frac{(\tilde{\lambda}_s t_s - \tilde{a}_s m_{S_R}^2)^2}{m_{S_R}^2 (m_{S_R}^2 + \tilde{\lambda}_s v^2)^2}. \quad (42)$$

We show in Fig. 1 how the various constraints determine the physically interesting region of parameter space. As emphasized before, the vacuum structure depends only on four microscopic parameters: λ_s , $m_{S_R}^2$, t_s and M_{D_1} (if A_s can be neglected). We show a projection on the t_s - λ_s plane (note that we use the microscopic λ_s , not the effective $\tilde{\lambda}_s$), for fixed $M_{D_1} = 35$ GeV and $m_{S_R}^2 = (100 \text{ GeV})^2$. In this figure we neglect the temperature dependence in \tilde{m}_s^2 and \tilde{t}_s , just as was done in Ref. [19], but we will make no approximations in the numerical studies of subsequent sections. The light blue region (to the right of the boundary marked as “ ϕ_c exists”) corresponds to the condition $\phi_c^2 > 0$, which coincides with the condition $\lambda_{\text{eff}}|_{T=0} < 0$. The dashed line corresponds to the boundary where Eq. (42) is saturated, so that to the right of this line the theory does not break the EW symmetry. The interesting region then lies between the

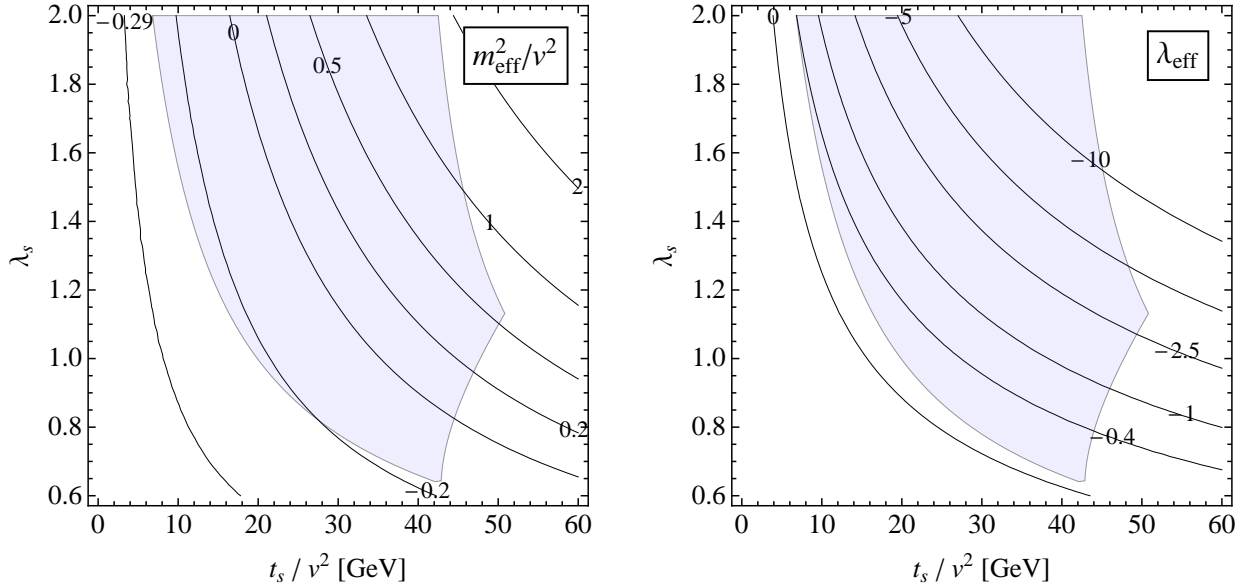


Figure 2: Left panel: lines of constant m_{eff}^2/v^2 , as defined by Eq. (32). Right panel: lines of constant λ_{eff} , as defined by Eq. (33). Both quantities are evaluated at $T = 0$. The shaded (light blue) region corresponds to that consistent with a strongly first-order EWPT and a heavy enough Higgs mass, for the same choice of parameters of Fig. 1.

two previous boundaries. In addition, we denote in a red shade the region where the EWPT is strongly first-order, as defined by the criterion $\phi_c/T_c > 1/\sqrt{2}$ (recall that our normalization is such that at $T = 0$, $\langle \phi \rangle = 174$ GeV). It is clear from the figure that the condition $\lambda_{\text{eff}}|_{T=0} < 0$ leads almost automatically to a strongly first-order EWPT. This point has been emphasized more generically in [42]. We have also indicated in green the region where the lightest CP-even Higgs has a mass $m_h > 114$ GeV, where

$$m_h^2 = \frac{1}{2} \left\{ \text{Tr} \mathcal{M}_H^2 - \sqrt{(\text{Tr} \mathcal{M}_H^2)^2 - 4 \text{Det} \mathcal{M}_H^2} \right\}, \quad (43)$$

and \mathcal{M}_H^2 is given in Eq. (20) (with $\delta = 0$). Although this condition is overly restrictive, since the lightest CP-even Higgs state has in general a singlet component, it illustrates that the Higgs LEP bound is easily consistent with a strongly first-order EWPT. It should be noted, however, that obtaining a heavy enough Higgs mass requires that the 1-loop radiative corrections be significant. In particular, in the $\tan \beta = \infty$ limit, the presence of the singlet does not affect the Higgs mass compared to the MSSM [see the expression for $\tilde{\lambda}$ in Eq. (29)]. However, it is also important that there is no need for either top scalar superpartner to be light in order to achieve a strongly first-order EWPT, unlike in the light stop scenario of the MSSM. Hence, both the LH and RH stops can be taken somewhat heavy. In the figure, we have chosen $m_{\tilde{t}_L} = m_{\tilde{t}_R} = M_{\text{SUSY}} = 2$ TeV. The hatched region corresponds to models that exhibit a strongly first-order EWPT *and* are allowed

by the LEP Higgs bounds. The shape of the allowed region is similar for other choices of M_{D_1} and $m_{S_R}^2$. However, as we will see, there are further constraints coming from the neutralino/chargino sector (in connection to DM) that prefer relatively small values for M_{D_1} . Note also that λ_s is required to be sizable although, as we will see, DM constraints have a preference for the lower range of values.

In Fig. 2 we show again the allowed region, for the same parameters of Fig. 1, and superimpose the lines of constant $m_{\text{eff}}^2/v^2|_{T=0}$ (left panel) and $\lambda_{\text{eff}}|_{T=0}$ (right panel). This shows that the allowed region is indeed characterized by $\lambda_{\text{eff}}|_{T=0} < 0$, as well as moderate $m_{\text{eff}}^2|_{T=0}$ in the sense that the effective mass parameter is at most of order v^2 (it is also clear that this does not represent an overly restrictive condition). It can also be checked that the allowed region satisfies $G_{\text{eff}}m_{\text{eff}}^2/\lambda_{\text{eff}}^2|_{T=0} \lesssim 0.9$, thus validating the physical picture described in the paragraph before Eq (40).

5 Pseudo-Dirac Dark Matter - Constraints and Signals

We now discuss various aspects of Dark Matter physics in detail. We assume that the scale of supersymmetry breaking is high enough that the lightest R -parity odd superpartner, which is a DM candidate, is a WIMP –usually the lightest neutralino.¹⁰ This is in contrast to models with low-scale supersymmetry breaking where the gravitino is likely the DM candidate. Thus, the relic abundance of the DM candidate is determined by a freeze-out calculation,¹¹ and the LSP is also expected to be seen in direct-detection experiments. In the $U(1)_R$ symmetric limit, the neutralino is Dirac in nature and scatters with nuclei either via s -channel squark exchange if it is gaugino like, or via t -channel Z -exchange if it has an appreciable Higgsino component, through a vector-vector interaction which is *not* suppressed by the DM velocity. As such, these contributions are subject to extremely stringent constraints. Hence, a Dirac neutralino DM candidate is essentially ruled out.

However, in the presence of (small) R -violating operators which are necessarily present, the two degenerate mass eigenstates of the Dirac DM split into two Majorana fermions with (slightly) non-degenerate masses. Hence the DM in this framework is *pseudo-Dirac* in nature. This can naturally allow for consistency with the latest direct-detection constraints from XENON100 [43] if the splitting between the eigenstates is larger than the typical momentum transfer (of $\mathcal{O}(100)$ keV) in a direct-detection experiment, such that the transition from one state to the other is kinematically forbidden. In our framework, we assume that the R -breaking

¹⁰Note that R -parity is still conserved in the model even when $U(1)_R$ is broken by Majorana gaugino masses and/or the $B\mu$ term.

¹¹Assuming a standard radiation-dominated era after the end of inflation until after BBN.

is such that the two Majorana eigenstates are split by $\delta m > 100$ keV (typically a few GeV, which could arise from anomaly mediation for example). Thus, the pseudo-Dirac DM is Majorana-like for the purposes of direct-detection. Note that this is quite different from the scenario of inelastic DM (iDM) [44], where the two states are split by an amount comparable to the momentum transfer in direct detection experiments. The situation regarding relic abundance can be completely different, however, since the freeze-out temperature T_F of the LSP (of $\mathcal{O}(1-10)$ GeV for a WIMP) is much larger than the typical momentum transfer in direct-detection. Thus, as long as $\delta m \lesssim T_F$, which can naturally occur in our framework, the DM properties are similar to those of a Dirac particle in regards to the relic abundance, as a result of coannihilation processes being in equilibrium.

5.1 Relic Abundance

As mentioned earlier, we assume for concreteness that the universe passes through a “standard” radiation dominated era beginning from a high temperature due to reheating after inflation, which persists until the time of matter-radiation equality. The relic abundance of a WIMP DM candidate is then determined by a thermal freeze-out calculation. The annihilation channels relevant for computing the relic abundance of DM after freeze-out can be divided broadly into three classes: a) annihilation into fermions, b) annihilation into Higgs/ W/Z states, and c) annihilation into gluon/photon final states.

What can be said about the above channels within the class of models considered? The region of parameter space consistent with a strongly first-order EWPT and LEP bounds for Higgs and chargino masses (as well as the direct detection constraints to be discussed in the next subsection), typically gives rise to a DM candidate with a mass such that the annihilation channels in (b) above are kinematically forbidden or suppressed. Furthermore, since DM is supposed to be neutral with respect to electric charge and color, DM annihilation channels in (c) occur via loop effects which may become important only when the annihilation channels in (a) are suppressed, such as due to helicity suppression for s -wave annihilation of Majorana DM.

Therefore, for the pseudo-Dirac DM with $\delta m \lesssim T_F$, arising in the scenarios considered in this work, only s -wave annihilation into fermion final states is relevant, which will be assumed from now on. This class of annihilation channels can be further subdivided into three types depending upon the particle exchanged in the s or t channel. Thus, the annihilation to fermion final states ($f\bar{f}$) may proceed through squark/slepton exchange, Z exchange, or Higgs exchange. Since the squark/slepton exchange contribution depends on their (model-dependent) masses and does not qualitatively affect any other aspect of the physics considered in this paper, we assume that the masses of squarks/sleptons are heavy enough such that their contribution to the relic abundance is subdominant and can be neglected. Furthermore, the Higgs exchange contribution

is suppressed by the masses of the fermions,¹² hence the dominant s -wave annihilation mode is through Z -exchange. The Z -exchange contribution is really a co-annihilation contribution since χ_1^0 and χ_2^0 (the two semi-degenerate Majorana states forming the pseudo-Dirac DM candidate) co-annihilate through a Z into fermion pairs in an s -wave process. Also, since only the Higgsino components of χ_1^0 and χ_2^0 couple to the Z , the relic abundance of the LSP is correlated with its Higgsino component. This can be seen more concretely by considering the pure Dirac (R -symmetric) limit. The coupling of Z to ψ_1 (the lightest Dirac neutralino in four-component notation) is given by:

$$\left(\frac{\sqrt{g^2 + g'^2}}{2} \right) Z_\mu \bar{\psi}_1 \gamma^\mu (c_L P_L + c_R P_R) \psi_1, \quad (44)$$

where $c_L = |U_{\psi_1 \tilde{H}_d}^L|^2$ and $c_R = |U_{\psi_1 \tilde{H}_u}^R|^2$, with U_L and U_R the unitary matrices diagonalizing the Dirac neutralino mass matrix, Eq. (21), i.e $U_L \mathbf{X}_N U_R^\dagger = \mathbf{diag}(m_{\psi_i})$. Thus, c_L and c_R correspond to the \tilde{H}_d and \tilde{H}_u components of ψ_1 , respectively. For a pure Dirac neutralino, the thermally averaged vector-vector annihilation cross-section to fermions arises from the vector piece of (44), and is given in the non-relativistic limit by:

$$\langle \sigma v \rangle_{Z\text{-exch}}^{\bar{\psi}_1 \psi_1 \rightarrow \bar{f} f} \approx \left(\frac{C^4}{2\pi} \right) \frac{m_{\psi_1}^2}{(4m_{\psi_1}^2 - m_Z^2)^2}, \quad (45)$$

where we defined

$$C^4 = \left(\frac{\pi^2 \alpha^2}{c_W^4 s_W^4} \right) (c_L + c_R)^2 \sum_i g_{f_i}^2. \quad (46)$$

The sum runs over all SM (Weyl) fermions lighter than ψ_1 (typically including the bottom, but not the top quark), and $g_{f_i} = T_{f_i}^3 - 2s_W^2 Q_{f_i}$ is the standard coupling of f_i to the Z gauge boson. We neglected phase space suppression factors that are very small even for the bottom quark, for the typical neutralino masses of interest. This expression is modified slightly when R -breaking is included, so that the process now corresponds to co-annihilation of χ_1^0 and χ_2^0 , the masses of which are split by δm . In the limit that $\delta m \ll m_{\psi_1}$, we can write approximately

$$\begin{aligned} \langle \sigma v \rangle_{Z\text{-exch}}^{\chi_1 \chi_2 \rightarrow \bar{f} f} &\approx \langle \sigma v \rangle_{Z\text{-exch}}^{\bar{\psi}_1 \psi_1 \rightarrow \bar{f} f} \frac{2}{g_{\text{eff}}^2} (2 + \delta)^2 (1 + \delta)^{3/2} e^{-x_F \delta}, \\ g_{\text{eff}} &= 2 + 2(1 + \delta)^{3/2} e^{-x_F \delta}; \quad \delta \equiv \frac{\delta m}{m_{\chi_1^0}}. \end{aligned} \quad (47)$$

Here $x_F = m_{\chi_1^0}/T_F$ with $m_{\chi_1^0} \approx m_{\psi_1}$ and T_F the freeze-out temperature of χ_1^0 and χ_2^0 , which has to be determined self-consistently.

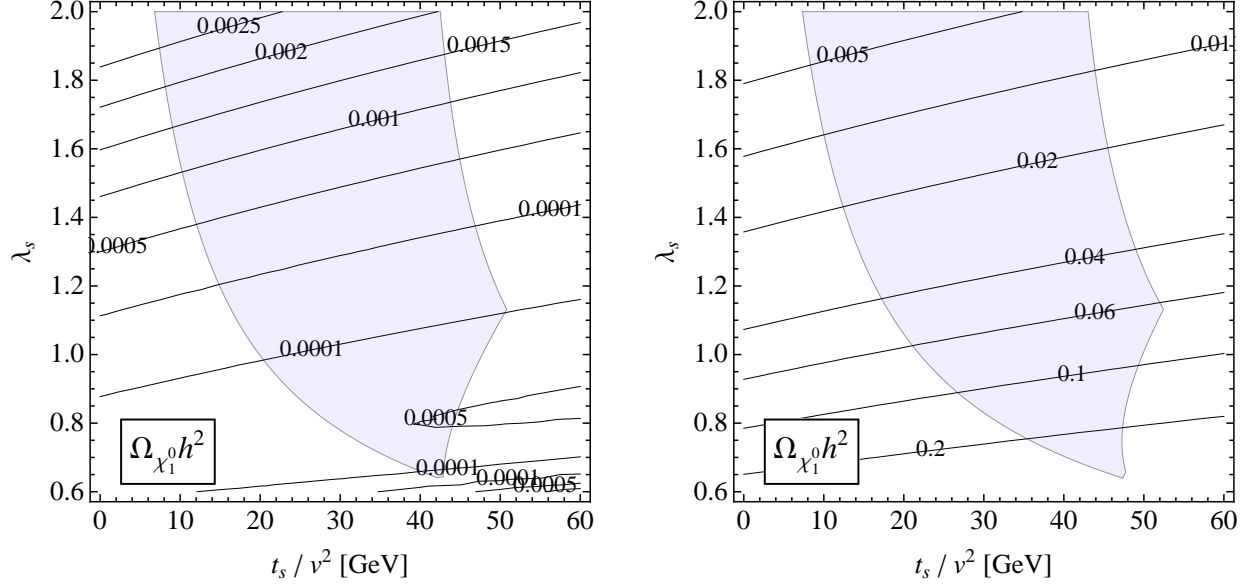


Figure 3: Contours of the LSP relic-abundance $\Omega_{\chi_1^0} h^2$ in the t_s - λ_s plane for the following choice of parameters. Left panel: $M_{D_1} = 35$ GeV, $M_{D_2} = -110$ GeV, $m_{S_R} = 100$ GeV, $M_{\text{SUSY}} = 2$ TeV; $M_1 = 5$ GeV, $M_2 = 10$ GeV, $b = B\mu = (40 \text{ GeV})^2$. Right Panel: $M_{D_1} = 60$ GeV, $M_{D_2} = -110$ GeV, $m_{S_R} = 100$ GeV, $M_{\text{SUSY}} = 2$ TeV; $M_1 = 10$ GeV, $M_2 = 20$ GeV, $B\mu = (40 \text{ GeV})^2$. The shaded (light blue) region in the plots corresponds to that consistent with a strongly first-order EWPT and a heavy enough Higgs mass (in the R -symmetric limit, which should not change much if the small R -violation due to b is also included in the minimization of the potential).

Fig. 3 shows contours of the LSP relic-abundance for two choices of parameters (see also Fig. 5 for further motivation for these choices). The LSP relic abundance in the left panel is always a small fraction ($\lesssim 1\%$) of the total DM abundance determined by WMAP [45]. However, the LSP relic abundance in the right panel is typically an $\mathcal{O}(1)$ fraction of the total DM abundance, and could even account for the *entire* relic abundance in a region of parameter space. The main reasons for the different relic abundances in the two plots above is the following. First, the LSP masses for the choice of parameters in the left panel are close to $m_Z/2$, as seen from the left panel of Fig. 4,¹³ causing a resonant enhancement in the annihilation cross-section. No such resonance enhancement is present in the right panel since the LSP masses are larger and essentially outside the “resonance” region (see right panel of Fig. 4). Also, the quantity δ in the left-panel is generically smaller than that in the right panel. Although, the precise value of $\delta \equiv (m_{\chi_2^0} - m_{\chi_1^0})/m_{\chi_1^0}$ varies throughout the plots, δ is roughly given by $M_1/m_{\chi_1^0}$, which is $\sim 1/9$ in the left panel and $\sim 1/6$ in the right panel above. Since the relic abundance depends exponentially on δ through Eq. (47), and $x_F \sim 25$, this also has a non-trivial effect on the relic

¹²The DM is typically not heavy enough to annihilate into $t\bar{t}$.

¹³Fig. 4 also illustrates that the mass of the lightest neutralino (LSP) for these two choices of parameters is consistent with the LEP bound on the invisible Z -width. The lightest chargino mass ($\gtrsim 105$ GeV) for these choices of parameters is also above the direct LEP bound.

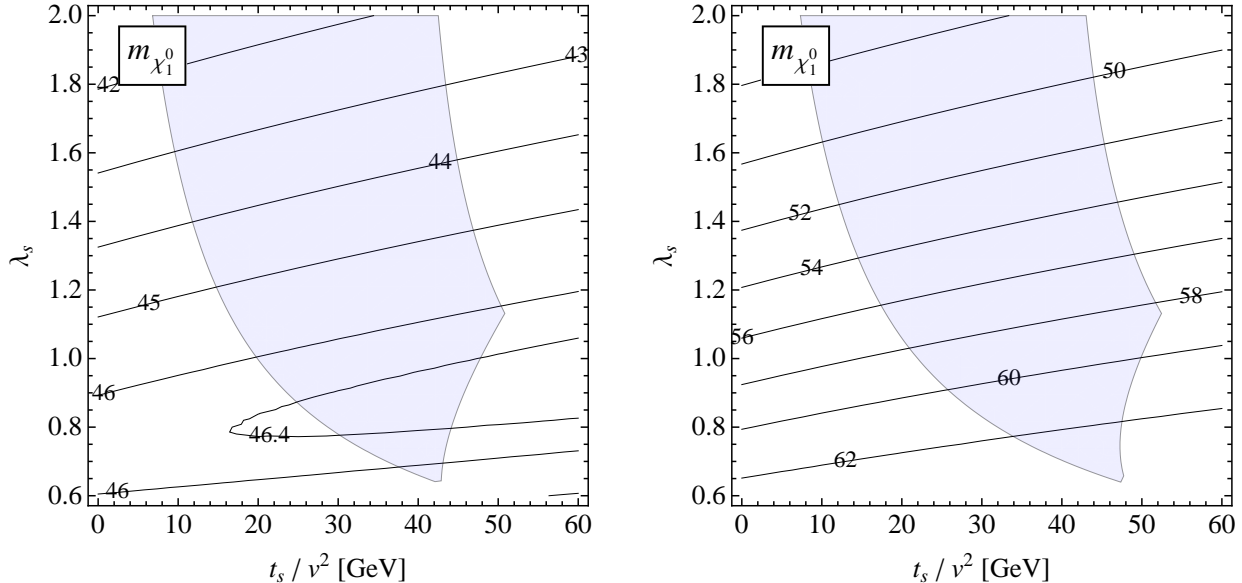


Figure 4: Contours of the lightest neutralino (DM candidate) mass in the t_s - λ_s plane for the two choices of parameters of Fig. 3. The shaded (light blue) region corresponds to that consistent with a strongly first-order EWPT and a heavy enough Higgs mass, in the R -symmetric limit.

abundance. Hence, demanding that the LSP abundance accounts for all the DM in the Universe favors a relatively “large” value of δ , implying a relatively “large” amount of R -breaking. However, since the R -breaking is technically natural,¹⁴ all effects arising from the breaking of the R -symmetry are naturally suppressed by powers of δ and loop factors. Furthermore, R -breaking by Majorana gaugino masses does not affect the scalar potential and hence the shape of the shaded (light blue) region in the figures at leading order.

5.2 Direct Detection

Having established that the LSP relic density can be a sizable fraction of the energy content of the universe, we now turn to its detection. Since the pseudo-Dirac LSP behaves like a Majorana particle for direct detection, the two main channels through which it can scatter off a nucleon is through an axial-vector interaction or a scalar-scalar interaction. The axial-vector interaction goes like v^2 , where v is the present velocity of DM in the surrounding halo ($\sim 10^{-3}c$); hence, the dominant interaction is via a scalar-scalar interaction, through Higgs exchange. The Higgs exchange contribution arises only if the lightest neutralino has a non-trivial Higgsino component.

What is the typical size of the Higgsino component in our framework? The parameter space for a non-trivial Higgsino component is correlated with that giving rise to a strongly first-order

¹⁴In the sense that one has an enhanced symmetry in the limit when the coefficients of the R -breaking operators vanish.

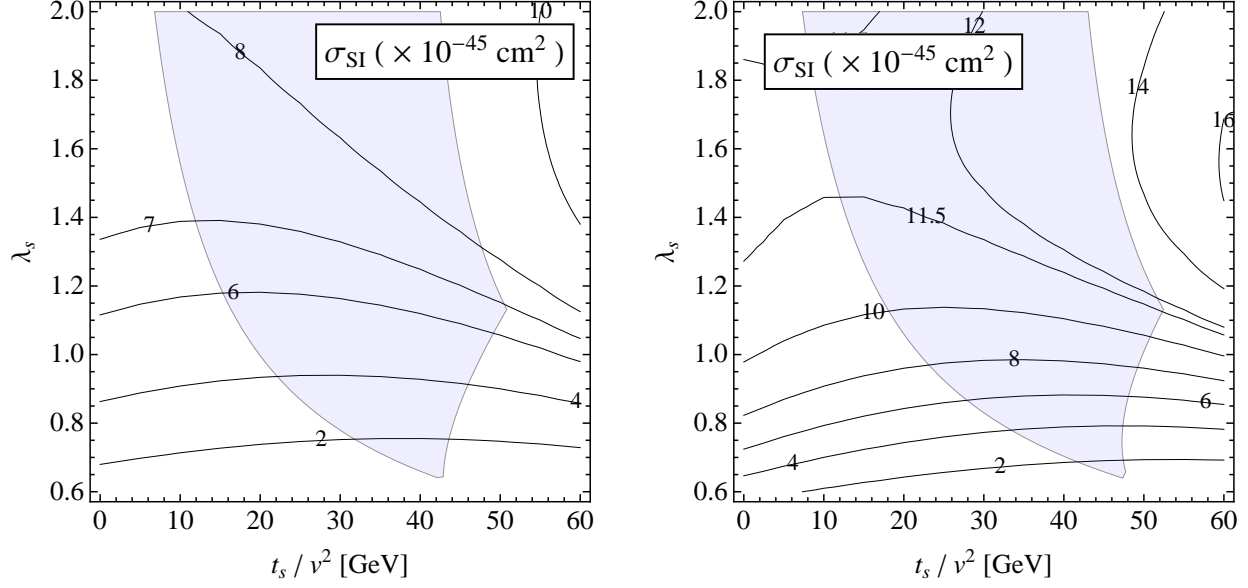


Figure 5: Contours of the spin-independent direct detection cross-section (in units of 10^{-45} cm^2) in the t_s - λ_s plane for the following choice of parameters. Left panel: $M_{D_1} = 35 \text{ GeV}$, $M_{D_2} = -110 \text{ GeV}$, $m_{S_R} = 100 \text{ GeV}$, $M_{\text{SUSY}} = 2 \text{ TeV}$; $M_1 = 5 \text{ GeV}$, $M_2 = 10 \text{ GeV}$, $B\mu = (40 \text{ GeV})^2$. Right Panel: $M_{D_1} = 60 \text{ GeV}$, $M_{D_2} = -110 \text{ GeV}$, $m_{S_R} = 100 \text{ GeV}$, $M_{\text{SUSY}} = 2 \text{ TeV}$; $M_1 = 10 \text{ GeV}$, $M_2 = 20 \text{ GeV}$, $B\mu = (40 \text{ GeV})^2$. The shaded (light blue) region in the plots corresponds to that consistent with a strongly first-order EWPT and a heavy enough Higgs mass, in the R -symmetric limit.

EWPT in the model. This can be understood as follows. Fig. 1 shows that the existence of a strongly first-order EWPT with a heavy enough Higgs mass to satisfy the LEP bounds requires $\lambda_s \gtrsim 0.6$. However, it turns out that the coupling of χ_1^0 to h_u^0 , which is the Higgs state with SM couplings to nucleons, increases as one increases λ_s . Since the χ_1^0 - h_u^0 coupling is given by

$$U_{\chi_1^0, h_u^0} = \left(-\frac{g}{\sqrt{2}} U_{\tilde{W}} + \frac{g'}{\sqrt{2}} U_{\tilde{B}} \right) U_{\tilde{H}_u} + (\lambda_s U_{\tilde{S}} + \lambda_T U_{\tilde{T}}) U_{\tilde{H}_d}, \quad (48)$$

where U_a corresponds to the “ a ” component of χ_1^0 , $U_{\chi_1^0, h_u^0}$ is linearly related to the Higgsino components of the LSP, i.e. $U_{\tilde{H}_u}$ and $U_{\tilde{H}_d}$. Therefore, the lower bound on λ_s for a strongly first-order EWPT places a lower bound on the Higgsino components of DM, thereby implying a lower bound on the Higgs-exchange spin-independent direct-detection cross-section, σ_{SI} .

Taking into account the exchange of the two CP-even Higgses with couplings to fermions, the spin-independent nucleon/DM elastic scattering cross-section can be written, in the non-relativistic limit, as

$$\sigma_{\chi_1^0}^{\text{SI}} \approx \frac{4U_{\chi_1^0, h_u^0}^2 g_{\text{hNN}}^2}{\pi} \frac{m_N^2 m_{\chi_1^0}^2}{(m_N + m_{\chi_1^0})^2} \frac{(U_{H, h_u}^2 m_h^2 + U_{h, h_u}^2 m_H^2)^2}{m_H^4 m_h^4}, \quad (49)$$

where h and H are the CP-even Higgs mass eigenstates that have an h_u^0 component [see Eq. (20)].

Here \mathbf{U} denotes the unitary matrix that diagonalizes the $\{h_u^0, s\}$ system and $\mathbf{U}_{h,h_u}^2, \mathbf{U}_{H,h_u}^2$ denote the h_u^0 content in h and H , respectively. We also have that the effective Higgs-nucleon coupling is $g_{hNN} \approx 0.3(gm_N)/(2m_W)$, with m_N the nucleon mass [46]. In Fig. 5, we show the contours of constant $\sigma_{\text{SI}} = \sigma_{\chi_1^0}^{\text{SI}}$ for the two different choices of parameters for which we showed the relic density in the previous section. Since the Majorana nature of DM is crucial for direct detection bounds, the set of parameters includes R -breaking Majorana gaugino masses and the $B\mu$ parameter (these were also included in the relic density contours). The shaded (light blue) region is, however, drawn in the R -symmetric limit for simplicity, as the small R -breaking has a minimal effect on the size and shape of this region.

Fig. 5 shows that a subset of the shaded (light blue) region is consistent with the latest XENON100 upper bound ($7 \times 10^{-45} \text{ cm}^2$ for $M_{DM} \approx 50 \text{ GeV}$) for both choices of parameters. The allowed region is smaller in the right panel of the figure compared to the left one, mainly because U_{11} is larger for the choice of parameters in the right panel compared to that for the left, and because the lightest Higgs mass is approximately equal in both plots. However, it is worth noting that due to the lower bound on the direct-detection cross-section in the model, as illustrated in the plots, it is expected that the next round of results from XENON100 should be sensitive to this class of models, *especially if the LSP accounts for an $\mathcal{O}(1)$ fraction of DM*. If, on the other hand, the LSP accounts for a negligible fraction of DM, then the detectability of the signal depends on the product $\rho_{\text{local}}^{\text{LSP}} \sigma_{\text{SI}}$ since it is this combination which determines the rate at a direct-detection experiment.¹⁵

Discussion: It is important to properly interpret the plots in Figs. 3 and 5 showing the results for relic-abundance and direct-detection. The point to note and appreciate is that depending on where one sits in the parameter space, the relic abundance and the expected signal for direct detection can vary considerably. One possibility, as seen from the plots in the right panels of Figs. 3 and 5, is that the LSP of the model accounts for the entire DM relic abundance and also provides a signal in the next round of direct-detection experiments. However, it is perfectly possible that the LSP abundance is a small fraction of the DM relic abundance as seen in the left panel of Figs. 3. This would imply that the dominant component of DM has a different origin. However, a direct-detection signal is nevertheless possible in this case if σ_{SI} is large enough (greater than the XENON100 bound of $7 \times 10^{-45} \text{ cm}^2$ for $m_{DM} = 50 \text{ GeV}$) and the local LSP abundance in the halo is appreciable, since the experiments are only sensitive to the product $\rho_{\text{local}}^{\text{LSP}} \sigma_{\text{SI}}$. Fig. 5 shows that large SI cross-sections are possible. Similarly, an indirect-detection signal in the form of cosmic-ray neutrinos from the sun for LSPs with a small relic abundance may be possible (see next subsection).

The LSPs could also provide an $\mathcal{O}(1)$ fraction of DM, so that DM consists of more than one

¹⁵ $\rho_{\text{local}}^{\text{LSP}}$ is the density of the LSP at the Earth's position.

non-negligible components. For example, axions provide an elegant solution to the strong CP-problem and also provide a good candidate for DM. They also naturally arise within string theory. Hence, it is a natural possibility that both WIMPs and axions provide an $\mathcal{O}(1)$ contribution to the total DM in the Universe. In fact, it has been shown that this can occur in well-motivated particle physics frameworks arising from string theory [47, 48]. Finally, the plot in the right panel of Fig. 3 shows that it is also possible for the LSP abundance to be *larger* than the total relic abundance. However, the implicit assumption in these plots is that the contribution from the annihilation channels mediated by t -channel squark/slepton exchange is negligible. The above assumption is relaxed if the squarks/sleptons are light enough, so that these regions may also become viable in that situation (as we will discuss in Section 7, light sfermions can be consistent with EWBG and bounds on EDMs).

Thus, even if the above framework provides a correct description of electroweak scale physics, the precise region of parameter space selected by Nature can only be determined by detailed measurements from a combination of experiments and observations in particle physics and astrophysics.

5.3 Indirect Detection

In addition to “directly” detecting the WIMP DM candidate by its recoil when it scatters with nuclei in a detector, another possible observable signal of WIMPs arises from the production of electrons, positrons, antiprotons, photons and neutrinos from LSP annihilation inside the Galactic Halo. This “indirect” detection of DM has received a lot of attention in recent years following the results of PAMELA [49] and FERMI [50].

What are the prospects for indirect detection within our framework? The WIMP DM candidate in the allowed region of parameter space tends to be light, i.e $m_{\chi_1^0} \lesssim m_W$. Also, although during freeze-out, χ_1^0 acts like a (pseudo) Dirac particle,¹⁶ it acts like a Majorana particle at present since the kinetic energy of χ_1^0 is not enough to overcome the mass difference between χ_1^0 and χ_2^0 . Therefore, the dominant co-annihilation contribution to the cross-section giving rise to the relic-abundance in Fig. 3 is not operative. It follows that the signal for cosmic ray electrons and positrons is significantly below that seen by PAMELA or FERMI. The PAMELA and FERMI signal must have a purely astrophysical interpretation within this framework. A similar statement holds for cosmic γ -rays produced by $\chi_1^0 \chi_1^0$ annihilations. The DM annihilation signal is too weak to explain the γ -rays observed by FERMI [51], hence those should have a purely astrophysical explanation as well.

¹⁶In the sense that kinetic energy of χ_1^0 during the freeze-out era is large enough to allow χ_1^0 and χ_2^0 to co-annihilate.

What about cosmic ray neutrinos? Here, the situation is qualitatively different for a number of reasons. As the solar system moves in the galactic halo, the WIMPs occasionally scatter with the nuclei in the sun and can lose momentum and become gravitationally bound with it. For a wide-range of choices of interaction parameters, an equilibrium can be established between the annihilation and capture rate over the lifetime of the sun. Among the various annihilation products of WIMPs inside the sun, neutrinos are unique since only they can travel to the earth without significant absorption. Another important difference between indirect detection via neutrinos and via other cosmic rays such as photons or electrons is that the signal depends *not* on the annihilation cross-section $\langle\sigma v\rangle$, but on the spin-independent (SI) and spin-dependent (SD) scattering cross-sections with nuclei (H and He in the sun).¹⁷

Since the neutrino signal depends on both SI and SD cross-sections and there are very stringent bounds on the SI cross-section from XENON100, having a large SD cross-section is crucial for a detectable signal. The effective operator (in four-component notation) and SD scattering cross-section against nucleons arising from t -channel exchange of Z bosons is [52]:

$$\begin{aligned}\mathcal{L}_{\chi_1}^{\text{SD}} &= b_q^A (\bar{\chi}_1^0 \gamma^\mu \gamma^5 \chi_1^0) (\bar{q} \gamma_\mu \gamma^5 q) , \\ b_q^A &= -T_q^3 V_{11} \left(\frac{e^2}{4s_W^2 c_W^2 m_Z^2} \right) , \quad V_{11} = |U_{\tilde{H}_d}|^2 - |U_{\tilde{H}_u}|^2 , \\ \sigma_{\chi_1^0}^{\text{SD}} &\approx \frac{24}{\pi} G_F^2 \frac{m_N^2 m_{\chi_1^0}^2}{(m_N + m_{\chi_1^0})^2} a_N^2 ,\end{aligned}\tag{50}$$

$$\tag{51}$$

where using the results in [52], one finds approximately $a_p \approx 0.705 V_{11}$, $a_n \approx -0.555 V_{11}$, leading to $\sigma_{\chi_1^0, p}^{\text{SD}} \approx 1.77 \times 10^{-37} V_{11}^2 \text{ cm}^2$. Since χ_1^0 in the allowed region has a non-negligible Higgsino component which couples to the Z , V_{11} is an $\mathcal{O}(1)$ number giving rise to $\sigma_{\chi_1^0, p}^{\text{SD}} \gtrsim 10^{-39} \text{ cm}^2$. The typical SD cross-section in the allowed region is much larger than the SI cross-section ($\sigma_{\chi_1^0, p}^{\text{SI}} \lesssim 10^{-44} \text{ cm}^2$) because the latter is dominated by Higgs exchange. Relative to the SD-cross section, the SI contribution is suppressed by two powers of the small effective coupling of the Higgs to the nucleon, $g_{\text{hNN}} \sim 10^{-3}$. Since the LSP mass within the framework is expected to be $\lesssim m_W$, the relevant constraints come from Super-K [53], which can be satisfied. Also, within the framework the channels leading to copious neutrino production (W^+W^- , $\tau^+\tau^-$, $t\bar{t}$) [54] are not expected to be significant for the same reason. Following [55], and the projected sensitivity of the IceCube/DeepCore experiment [56], however, it is expected that this class of models should be observable in the near future in neutrino telescopes, if the LSP forms an $\mathcal{O}(1)$ fraction of DM. As for direct detection, if the LSP is a negligible fraction of DM, then its detectability crucially depends on the combination which appears in the capture rate: $(\rho_{\text{local}}^{\text{LSP}} \sigma_{\chi_1^0, H}^{\text{SD}}) / m_{\chi_1^0}^2$.

¹⁷This is true if the capture and annihilation rates have reached equilibrium, which holds true in our models.

Until now we have focused primarily on the LEP and relic-abundance constraints, as well as on the signals in direct and indirect detection experiments. We will briefly discuss collider and gravitational wave signals for our scenario in Section 8, after considering the issue of complex phases in regards to EWBG and EDM constraints in Section 7.

6 A Benchmark Example

In this section we perform a numerical analysis of the EWPT and DM properties, without some of the approximations used in the previous sections. For instance, we fully take into account small R -violating terms ($B\mu$, M_1 and M_2 , though not A -terms), and various small $vevs$. We also include the effects of the temperature-dependent singlet terms [i.e. those proportional to c_{S2} and c_S in Eq. (27)]. However, we do not perform a full effective potential analysis, restricting rather to the thermal mass contributions at leading order. We also do not include CP-violating phases (see the next section for further discussion on this point).

For a given choice of parameters, we first minimize numerically the potential at zero temperature, and determine the spectrum of Higgses, neutralinos and charginos, as well as their composition. Only the dimensionless ratios of the dimensionful input parameters are meaningful, since we can always rescale them a posteriori to normalize to $v = 174$ GeV. We then consider the finite-temperature potential to find the critical temperature. In order to do so, we increase T , and look for all real extrema of the potential (which is just polynomial in the approximation we are using), identifying EW-preserving (where only S has a vev) and violating minima. We then compare the potential energies associated with these minima in order to identify the global one, for the given T . By iteration, we can then identify the critical temperature, defined by degeneracy of the EW symmetry preserving and violating minima. Note also that since we can take all squark and slepton soft masses to be positive and large (unlike in the MSSM, they do not play a role whatsoever in making the transition first-order), we do not need to worry about color- or charge-violating minima.

As an example, consider the set of parameters (in GeV units where relevant) given by

$m_{H_u}^2$	$m_{H_d}^2$	b	λ_s	t_s	B_s	m_s^2
$-(100)^2$	$(100)^2$	$(20)^2$	0.8	$(111)^3$	$-(100)^2$	$(125)^2$
λ_T	B_T	m_t^2	M_{D_1}	M_{D_2}	M_1	M_2
1	$(300)^2$	$(2000)^2$	60	-110	7.5	16

We also take $g \approx 0.65$, $g' \approx 0.35$ and $y_t \approx 1$, which results in $c_\phi \approx 0.92$, $c_{S2} \approx 0.24$ and $c_S \approx -2.78$ GeV, from Eqs. (26) and (27). For the zero-temperature radiative corrections

we use $M_{\text{SUSY}} = 2$ TeV. The zero-temperature Higgs $vevs$ are given by $v_u \approx 173.99$ GeV, $v_s \approx 62$ GeV, $v_d \approx 1.2$ GeV, $v_T \approx -7 \times 10^{-3}$ GeV. Note that $v_u/v_d \approx 150$, illustrating that in this framework “ $\tan \beta$ ” can be much larger than in the MSSM context (see next section). However, this ratio can easily be changed by changing b , which barely has an effect on the main physical properties of the model. Also, the triplet vev is sufficiently small to be irrelevant from the point of view of EW precision constraints.

The spectrum of CP-even (m_{H_i}), CP-odd (m_{A_i}) and charged ($m_{H_i^\pm}$) Higgses, in GeV, is

m_{H_1}	m_{H_2}	m_{H_3}	m_{H_4}	m_{A_1}	m_{A_2}	m_{A_3}	$m_{H_1^\pm}$	$m_{H_2^\pm}$	$m_{H_3^\pm}$
116	184	245	2060	234	245	1960	129	1960	2060

while the neutralino and chargino spectra are given by

$m_{\chi_1^0}$	$m_{\chi_2^0}$	$m_{\chi_3^0}$	$m_{\chi_4^0}$	$m_{\chi_5^0}$	$m_{\chi_6^0}$	$m_{\chi_1^\pm}$	$m_{\chi_2^\pm}$	$m_{\chi_3^\pm}$
63.2	70.7	107	120	241	244	107	127	270

It also of interest to note the composition of the two lightest neutral CP-even Higgses:

$$H_1 \sim 0.88 h_u^0 - 0.003 h_d^0 + 0.48 s - 0.003 T_R^3, \quad (52)$$

$$H_2 \sim 0.47 h_u^0 - 0.008 h_d^0 - 0.88 s + 0.005 T_R^3, \quad (53)$$

and of the LSP:

$$\chi_1^0 \sim 0.67 \tilde{b} + 0.12 \tilde{w}^3 + 0.05 \tilde{H}_d^0 + 0.35 \tilde{T}^3 - 0.54 \tilde{S} - 0.35 \tilde{H}_u^0. \quad (54)$$

The content of χ_2^0 is very similar due to the pseudo-Dirac nature of the neutralinos. For this parameter point, we find that the relic density is $\Omega_{\chi_1^0} h^2 \approx 0.11$, in accord with the WMAP constraint [45], while the LSP spin-independent cross-section is given by $\sigma_{\chi_1^0 N \rightarrow \chi_1^0 N} \approx 4.5 \times 10^{-45}$ cm², somewhat below the current XENON100 limit [43].

Turning now to the finite-temperature analysis, we find that the critical temperature is $T_c \approx 71.0$ GeV, while $v_c/T_c \approx 1.34$, exhibiting a strongly first-order EWPT, even when taking into account the points made in [57]. For comparison, the analytic formulas given in Section 4 give $T_c^{\text{analytic}} \approx 62.5$ GeV, while $(v_c/T_c)^{\text{analytic}} \approx 1.86$. The difference arises from the temperature-dependent singlet terms proportional to c_{S^2} and c_S . Nevertheless, we see that the physics is correctly captured by the simplified analysis. These results will shift slightly under a more detailed full effective potential analysis, but we do not expect that the conclusions will radically change.

7 \mathcal{CP} Phases - EWBG and EDM's

In Sections 3 and 4 we studied the scalar potential in the case that all the relevant parameters are real. This allows for a transparent understanding of the mechanism behind a strongly first-order phase transition, and its connection to the DM sector, that is typical in the scenarios we consider, as discussed in the previous sections. However, the production of a baryon asymmetry during the EWPT requires CP-violating phases. A complete treatment of this question, namely a study of the CP-violating sources that enter in the transport equations, their diffusion in front of the bubble wall, the communication of CP-violation to the LH quark sector and the subsequent processing by sphalerons, is beyond the scope of this work. Nevertheless, we will make a few remarks in connection to the production of the BAU that suggest that a large enough baryon asymmetry can be induced, while being easily consistent with the currently null EDM searches.

To be definite, we will frame our discussion in the context of “approach IV” described in Section 2, and discussed in more detail in Appendix B. We consider initially the exact $U(1)_R$ symmetric limit. The model contains four Higgs doublets (H_u, H_d, H'_u, H'_d , of which only H_u and H'_d acquire non-zero *vevs*), a SM singlet S , a $SU(2)_L$ triplet T , and a $SU(3)_C$ octet O . The superpotential and the soft breaking terms are given by Eqs. (64) and (65) of Appendix B, to which one adds the “supersoft” operators [see Eq. (5)] $iM_{D_a}\lambda_a\tilde{\Sigma}_a + \sqrt{2}M_{D_a}D_a\Sigma_a + \text{h.c.}$, where $\lambda_1 = \tilde{B}$, $\lambda_2 = \tilde{W}$, $\lambda_3 = \tilde{g}$, $\Sigma_1 = S$, $\Sigma_2 = T$ and $\Sigma_3 = O$, and the D_a are the auxiliary fields in the SM vector superfields. For simplicity, we have focused on a limit where H'_u and H'_d are somewhat heavier than the weak scale (due to a large μ' -term) and can effectively be integrated out.¹⁸ However, we will keep them below initially in order to count all possible phases more transparently.

The physical phases in the model, associated to the Higgs sector, are given by

$$\text{Arg}(t_s M_{D_1}^*) , \quad \text{Arg}(B_s M_{D_1}^{*2}) , \quad \text{Arg}(B_T M_{D_2}^{*2}) , \quad \text{Arg}(B_O M_{D_3}^{*2}) , \quad (55)$$

$$\text{Arg}(\lambda_S \mu^*) , \quad \text{Arg}(\lambda_T \mu^*) , \quad \text{Arg}(\lambda'_s \mu'^* b') , \quad \text{Arg}(\lambda'_T \mu'^* b') . \quad (56)$$

It is convenient to choose M_{D_a} to be real (by redefining the S, T and O superfields). Also, the phase of b' can be absorbed in H'_d , for instance, and then we can choose μ and μ' to be real by rephasing the H_d and H'_u superfields. Thus, we can choose the physical phases to reside in $\lambda_s, \lambda'_s, \lambda_T, \lambda'_T, t_s, B_s, B_T$ and B_O . The octet fields play no role during the phase transition, so we can

¹⁸Such a limit need not be essential to reach our conclusions: for instance, even if the primed Higgses have masses at the EW scale, as long as their *vevs* are somewhat suppressed our analysis of the phase transition should remain as a reasonable approximation. As $\langle H'_d \rangle$ becomes larger (note that $\langle H'_u \rangle$ can remain small due to the approximate R -symmetry), the analysis will become more complicated, but we don't think the fact that the system can easily display a strongly first-order EWPT will change. Similarly, a connection to DM should remain, as well as the suppression of EDM's, as discussed below.

set B_O aside. Also, since the triplet vev is required to be small by EW precision constraints, any possible phase in B_T is likely to play only a minor role. In addition, given that $\langle H_d \rangle = \langle H'_u \rangle = 0$ (i.e. we take their squared soft masses to be sufficiently positive), and that we can integrate out the heavy H'_u and H'_d , the Higgs potential can be seen to depend only on $H_u^\dagger H_u$, $H_d^\dagger H_d$ and S (setting $T \approx 0$, together with the vanishing of the octet O and squark/slepton fields). It follows that non-vanishing phases in the microscopic parameters can only induce a phase in the singlet vev , while all the Higgs doublet $vevs$ either vanish, or can be taken to be real by an $SU(2)_L$ transformation.

The phases of λ_s and λ_T enter in the chargino and neutralino mass matrices [see Eqs. (21) and (22)], as does a possible phase in $\langle S \rangle$ (λ'_s and λ'_T do not enter, as long as the H'_u and H'_d superfields are somewhat heavy). The S vev gives an interesting effect, not present in the MSSM, when $\text{Arg}\langle S \rangle$ is spacetime-dependent. Such a case was considered in Ref. [41] in the context of the related model of Ref. [19] (which does not have the $U(1)_R$ symmetry, but whose tree-level potential has the same form as ours). For the purpose of generating the BAU, the most important source of CP-violation comes from the chargino sector, at second order in the gradient expansion (assuming no degeneracy). In Ref. [41], it was found that the effect of the spacetime-dependent singlet complex vev easily leads to a significant baryon-to-entropy ratio $\eta = n_B/s \propto \Delta\theta_s/(l_w T_c)$, where l_w is the bubble wall thickness (typically large compared to $1/T \sim 1/T_c$), and $\Delta\theta_s$ is the change in the phase of the singlet across the bubble wall. Thus, the phases in t_s and/or B_s can generate a significant baryon asymmetry within the framework via a chargino source with CP-violation arising from the *change* in the singlet phase, even if λ_s and λ_T are real.

As emphasized in the Introduction, some level of R-violation is generically expected once the gravitino mass is generated. In fact, we pointed out in Section 5 that small Majorana gaugino masses can play a crucial role in order for the LSP to fully account for the DM content of the universe. This suggests a second, qualitatively different possibility for generating the BAU. If all the phases in the Higgs potential vanish (as assumed in the analysis of Section 4), while the CP-violating phases arise only from the suppressed Majorana gaugino masses, M_a , one expects that the CP-violating sources will be proportional to $\text{Im}(M_a)/M_{D_a}$. Such a suppression might be welcome in regions where a too large baryon asymmetry is produced, as suggested by the results of [41]. It would be interesting to further study the detailed aspects of EWBG in the previous scenarios (note that the model studied in [41] required sizable gaugino Majorana masses).

The above mechanisms for generating CP-violating sources during the EWPT should remain operative in the context of “approach I” described in Section 2. However, there can exist differences between approaches I and IV when it comes to EDMs. In order to see this, it will be useful to first comment on “ $\tan\beta$ ”. We have assumed that the EW vev , v , is carried mostly by one

Higgs doublet (H_u^0), and therefore in a sense we are always considering a “large $\tan\beta$ ” scenario. As is well-known, in the MSSM one often finds observables that are $\tan\beta$ enhanced/suppressed. In particular, large $\tan\beta$ enhancements arise in the down sector when the *vev that gives rise to the down-type fermion masses* is much smaller than v . Such enhancements are, however, tied to how these masses are generated, as illustrated by the two operators in Eq. (4). If the down-fermion masses arise from the first operator (as in approach I with a small R -violating $B\mu$ -term being responsible for \mathbf{m}_d and \mathbf{m}_e), the situation is “MSSM-like” in regards to such enhancements. However, if the down-fermion masses arise from the second operator (as in approach I with the Dobrescu-Fox mechanism [29], or as in approach IV), then the *vev* of H_d is not related to the down Yukawa matrices, $\mathbf{y}_{d,e}$. Instead, the measured fermion masses always relate the Yukawa couplings to $v_u \approx v$, and the source of $\tan\beta$ enhancements disappears. Notice that, as in approach IV, the down masses may be ultimately connected to a small *vev* like v'_d (see Appendix B). Thus, one can define two different (large) *vev* ratios, v_u/v_d and v_u/v'_d . One may then wonder if the second ratio can play the role of the MSSM $\tan\beta$, but as we will see the R -symmetry prevents “ $\tan\beta$ enhanced” terms from appearing.

The above remarks will be useful when considering the issue of EDM’s, which we will first discuss in the context of approach IV. As emphasized in [24], the approximate $U(1)_R$ symmetry leads to a significant relaxation of the constraints from the electron and neutron EDM’s (see [15] for a review). The point is that, at one-loop order, the EDM’s induced by a squark/slepton and gluino/chargino/neutralino loop require LR mass mixing in the sfermion sector. In the MSSM and many variants, including the model of Ref. [19], these LR mixings arise from A -terms and the μ -term, the latter effect being $\tan\beta$ enhanced in the down-type sector. In our scenario the situation is different: the A -terms are at least loop-suppressed (if they arise from anomaly mediation), while the $U(1)_R$ symmetry forbids the “usual μ -term”, i.e. a superpotential term coupling the Higgses responsible for the up and down-type fermion masses (in our case $H_u H'_d$). The “ μ -terms” allowed by the $U(1)_R$ symmetry, $\mu H_u H_d$ and $\mu H'_u H'_d$, do not contribute to LR sfermion mixing, as long as H_d and H'_u do not acquire *vevs*. This holds even in the presence of (small) Majorana gaugino masses, as required by the DM relic abundance (discussed in Subsection 5.1). Note that such Majorana gaugino masses will induce, at one-loop order, a $b_{\mathbb{R}} H_u H_d$ term, with $b_{\mathbb{R}} \sim [\alpha_a M_a \mu / (2\pi)] \log(\Lambda/\mu)$ [29] where α_a is a SM fine-structure constant and Λ is a UV cutoff. Such a b -term induces in turn a very small R -violating *vev* for $\langle H_d \rangle \sim v_u b_{\mathbb{R}} / m_{H_d}^2$, that translates into *very small* LR sfermion mixings in the down sector. In addition, since the down-type fermions get their masses mostly from the H'_d *vev*, instead of H_d , such LR mixings do not carry any “ $\tan\beta$ ” enhancements. Thus, we conclude that there are no constraints from one-loop level EDMs in our scenario, even if the sfermion masses are light (~ 1 TeV). This can be contrasted to the case of pseudo-Dirac gauginos without the $U(1)_R$ symmetry, studied

in [58]: while the M_a/M_{D_a} suppression can be common to the generation of the BAU and EDM's, in the $U(1)_R$ models the additional LR suppression renders the associated EDM's completely harmless.¹⁹ Similarly, two-loop Barr-Zee-type diagrams [59], involving a chargino in the loop, are also expected to give a contribution to EDM's suppressed by M_a/M_{D_a} , and are therefore negligible. As pointed out in [24], the leading contribution to EDM's in $U(1)_R$ symmetric scenarios corresponds to the Weinberg three-gluon operator [60], $(w/3)G \cdot \tilde{G} \cdot G$, which could be observable in the near future if the relevant CP-violating phases are order-one. However, these phases are associated with the gluino/octet sector, and therefore are not closely connected to the relevant phases for EWBG. Also, if the relevant CP-violating phases responsible for the BAU arise from the Higgs sector, as discussed in the first EWBG scenario above (say with very small/real Majorana gaugino masses), the CP-violation is communicated to the SM fermion sector only at a high-loop order, hence it is unconstrained by EDM bounds.

We end this section by commenting on EDM's within “approach I”. If the down-type fermion masses arise at one-loop order as in [29],²⁰ then the situation is similar to approach IV described above, since the down-fermion masses effectively arise from the second operator in Eq. (4) [see discussion on $\tan\beta$ above]. If, on the other hand, the down-type fermion masses arise from a small H_d vev induced by a R -violating $B\mu$ -term, then one can expect large $\tan\beta$ enhancements in the one-loop induced EDMs, that may compensate the M_a/M_{D_a} suppression associated with the pseudo-Dirac nature of the gauginos. A more detailed study is then necessary to estimate the bounds on the sfermion masses, but one can nevertheless expect an improvement compared to the situation in the MSSM (see e.g. [61]). This conclusion also holds for EDM's induced at 2-loop order.

8 Other Experimental Signatures

As mentioned at the end of Subsection 5.2, a combined set of measurements from a variety of experiments in particle physics and astrophysics will be needed in order to fully test the framework and zoom in on the preferred region of parameter space. In addition to DM direct and indirect detection, or EDM measurements, this would include collider physics signals at the LHC and other future collider experiments, as well as a possible gravity wave signal arising from the

¹⁹We note that the pseudo-Dirac nature of the gauginos by itself may be sufficient to allow for a successful EWBG, while being consistent with EDM searches, for natural values of the sfermion masses: the singlet can be responsible for a strongly first-order phase transition, such that in spite of the M_a/M_{D_a} suppression of the CP-violating sources, a sizable BAU can be generated. At the same time, the 1-loop EDM's are suppressed by the same M_a/M_{D_a} factor, allowing for lighter sfermions than in the MSSM.

²⁰However, note that due to the suppression in the Majorana gaugino masses, which comes on top of the one-loop suppression, it may be necessary to take rather large values for μ in order to generate the bottom Yukawa coupling [29]. Thus, this scenario may require some fine-tuning in the Higgs sector.

strongly first-order EWPT. Although a comprehensive study of phenomenological consequences will have some model-dependence and is beyond the scope of this paper, we will attempt to outline the characteristic signatures of the framework which depend only on its crucial features.

8.1 Collider Signatures

The framework has a number of interesting collider signatures which can be probed at the LHC. Some of the signatures arise as a consequence of the broad features of the framework considered in this paper, while others arise as general consequences of the R symmetry and hence share signatures with other R -symmetric models considered in the literature. We will focus primarily on the former and only briefly mention the latter, directing the reader to the relevant papers for reference.

The class of models considered here have a characteristic spectrum. The lightest degrees of freedom consist of the lightest CP-even Higgs, and the lightest chargino and neutralino, with the lightest neutralino being the LSP. They all have masses $\lesssim 120$ GeV. The other Higgses, charginos and neutralinos generically are heavier, spanning a large range between around 150 to several hundred GeV. However, in order to satisfy the constraints on the T -parameter, the triplet scalars have to be quite heavy, in the multi-TeV range. What about squarks, sleptons and gluinos? Since the physics underlying electroweak baryogenesis and DM in this work is essentially independent of them, and given the lack of significant constraints from EDM bounds, the masses of these particles are quite unconstrained, and can range from a few hundred GeV to multi-TeV.

The lightest CP-even Higgs in the allowed region of parameter space generically has a non-trivial singlet component. Therefore, the LEP constraints on the Higgs mass are somewhat relaxed, the exact amount depending on the parameters in detail. Although there exist additional tree-level contributions to the Higgs quartic in a model with the coupling $\lambda_s S H_u H_d$, the extra contribution vanishes in the $v_d \rightarrow 0$ limit, implying that radiative corrections are important in raising the Higgs mass. It is more challenging to discover the lightest CP-even Higgs in this class of models than in the SM or in the MSSM, due to two main reasons. First, as mentioned above, the Higgs has a sizeable singlet component which reduces its coupling to gauge bosons and quarks. Second, the decay mode $h \rightarrow \chi_1^0 \chi_1^0$ is generically available, allowing the Higgs to decay invisibly with an appreciable branching ratio.²¹ In such a case, vector boson fusion is expected to provide the most effective search channel at the LHC [62]. On the other hand, the orthogonal, and heavier combination of h_u^0 and s (call it H), can have a sizable coupling to gauge bosons and to the top quark, and be in a range where its decay into W/Z pairs has a sizable

²¹The lightest Higgs is expected to be below the weak boson production threshold.

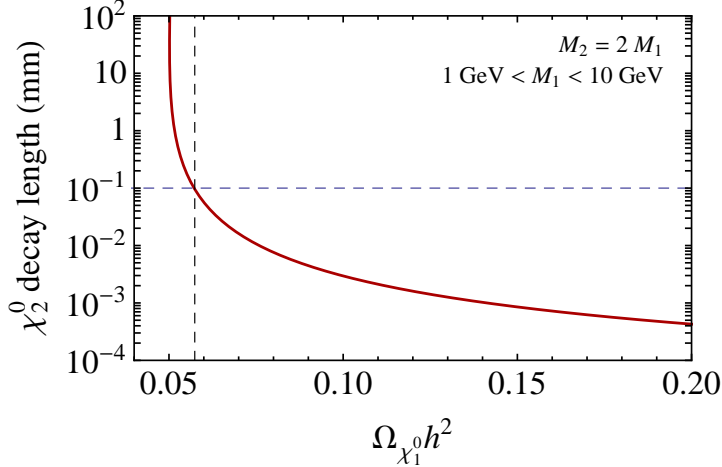


Figure 6: Correlation between the χ_2^0 rest frame decay length and the χ_1^0 relic abundance in the model of Section 6, as the $U(1)_Y$ Majorana gaugino mass, M_1 , is varied in the range $[1, 10]$ GeV. The dashed horizontal line indicates approximately the minimum decay length that is measurable.

branching fraction. Such a state may be looked for in $gg \rightarrow H \rightarrow WW/ZZ$. It hardly needs to be emphasized that Higgs physics in this framework is extremely rich and interesting, and should be thoroughly investigated.

The signatures related to the lightest neutralino and chargino are also very important since they are intricately tied to the DM physics. The lightest chargino in the allowed region tends to be close to the LEP bound; hence should be discovered at the LHC. What about the LSP? The pseudo-Dirac nature of the LSP gives rise to two quasi-degenerate states χ_1^0 and χ_2^0 split by a small amount δm , causing χ_2^0 to decay to χ_1^0 . Since $\delta m \ll m_{\chi_1^0}$, the decay length L could be large in some cases, leading to a displaced vertex. However, since $L \sim \delta m^{-5}$, the decay length is quite sensitive to δm and could span a large range.

Note that χ_2^0 decays to χ_1^0 and SM fermion pairs ($\bar{f}f$) through an operator which is precisely the same as the one relevant for computing the relic abundance of the LSP, *viz.* χ_1^0 and χ_2^0 co-annihilation to $\bar{f}f$ through Z -exchange! As observed in [63], if the χ_2^0 decay length is measurable, it allows for a non-trivial “measurement” of the relic density, solely based on collider data, that can then be compared to the cosmological observations. The point is that the χ_2^0 decay width, given by

$$\Gamma(\chi_2^0 \rightarrow \chi_1^0 f \bar{f}) \approx \frac{C'^4}{120\pi^3} \frac{\delta m^5}{M_Z^4}, \quad (57)$$

depends only on $\delta m = m_{\chi_2^0} - m_{\chi_1^0}$ and on a “coupling constant” C' which can be effectively identified with the constant C appearing in the annihilation cross-section, Eq. (46). The only difference is that the bottom quark contributes to C , but not to C' , which results in $C \approx 1.18C'$.

One can then see that there is a correlation between $\Omega_{\chi_1^0} h^2$ and the χ_2^0 decay length (given the two measurable quantities $m_{\chi_1^0}$ and δm) that is independent of the detailed composition of the LSP. A difference between our situation and that of Ref. [63] is that in our case the annihilation proceeds in the vicinity of the Z resonance, while in [63] both the annihilation and the decay width of the heavier pseudo-Dirac state were assumed to proceed via a very heavy state, leading to an effective contact interaction. As a result, we find that it is possible for the decay length to be macroscopic for pseudo-Dirac mass splittings that result in an *order one* relic density.

As an example, we show in Fig. 6 the χ_2^0 decay length versus $\Omega_{\chi_1^0} h^2$ in the benchmark example of Section 6. We only vary the Majorana gaugino masses, imposing for concreteness the “unified-like” relation $M_2 = 2M_1$, and letting $1 \text{ GeV} < M_1 < 10 \text{ GeV}$. In this range, the mass splitting between the two lightest neutralino states (with masses of about 60 GeV) varies as $0.85 \text{ GeV} \lesssim \delta m \lesssim 10 \text{ GeV}$. We then find that the χ_2^0 decay length in the rest frame is in the range $10 \text{ cm} \gtrsim L \gtrsim 0.5 \mu\text{m}$, and the relic density satisfies $0.05 \lesssim \Omega_{\chi_1^0} h^2 \lesssim 0.19$. Other properties, such as the strength of the phase transition, are not sensitive to the Majorana masses. Also, in the full range above, the spin-independent cross-section is consistent with current bounds. Thus, we see that $\mathcal{O}(1)$ relic abundances can be associated with observable ($\gtrsim 10^{-1} \text{ mm}$ [64, 65]) displaced vertices. Note that if the LSP is only one of several components of the total DM abundance, the above method (provided L is measurable) can give a very useful handle in determining its abundance. However, it is also possible that χ_2^0 is stable on collider time scales, in which case it could not be distinguished from the real LSP in a collider environment.

Before moving on to other signatures, we briefly mention some collider signatures which depend only on the existence of an approximate R -symmetry and are shared with other R -symmetric models in the literature. In the pure R -symmetric limit, it can be shown that cross-sections for many scattering processes, such as $qq' \rightarrow \{\tilde{q}_L \tilde{q}'_L, \tilde{q}_R \tilde{q}'_R\}$, $q\bar{q}' \rightarrow \{\tilde{q}_L \tilde{q}'_R, \tilde{q}_R \tilde{q}'_L\}$, $qg \rightarrow \{\tilde{q}_L \tilde{g}_D, \tilde{q}_R \tilde{g}_D\}$, and $g\bar{g} \rightarrow \{\tilde{g}_D \tilde{g}_D, \tilde{g}_D^c \tilde{g}_D^c\}$, vanish²² [66]. Thus, these scattering processes are suppressed if the R -breaking is small. The suppression of Majorana masses also implies suppression of same-sign lepton signals. In the Higgs sector, the presence of the R -charge 2 scalar H_d implies that it can only be pair-produced at colliders. At the LHC, Drell-Yan production mediated by weak gauge bosons is likely to be the dominant channel [67]. Also, in the R -symmetric limit each H_d decays to *two* neutralinos (with R -charge 1) giving rise to *four* neutralinos for events with pair-produced H_d 's. Finally, since the R -symmetric SSM can lead to a natural suppression of FCNCs even for $\mathcal{O}(1)$ flavor violating soft masses, the flavor violations in the soft mass-matrices can show up in variety of ways at the LHC [24], which is worthy of significant study.

²² \tilde{g}_D stands for the Dirac gluino.

8.2 Gravitational Waves

A strongly first-order EWPT proceeds by formation of bubbles of the broken phase which expand into the unbroken phase. Near the end of the phase transition, bubbles of the broken phase collide with each other, breaking the spherical symmetry and leading to production of gravitational waves [68]-[72]. Thus, a strongly first-order EWPT can give rise to gravitational waves, which are in principle observable by space-based interferometers like LISA or BBO.

A detailed study of the feasibility of observing a gravitational wave signal arising from the EWPT within our framework is beyond the scope of this paper, and we will limit ourselves to a few remarks. As explained in Section 4, the structure of the finite temperature potential within the framework is qualitatively different than in the MSSM or the SM, which naturally allows the possibility of a strongly first-order EWPT. The crucial feature is the presence of a barrier due to a negative effective quartic term in the effective potential, which is balanced by a “tower of operators” arising at higher order (see Eqs. (31)-(33) and the discussion below). It turns out that a stronger phase transition proceeds at a lower temperature and creates larger bubbles, shifting the peak of the gravity wave spectrum to lower frequencies, below the best sensitivity range of satellite experiments like LISA and BBO. However, as explained in [70], since the gravity wave spectrum has a much milder fall-off with frequency ($\sim f^{-1.0}$) than thought earlier [73], it is expected that BBO would be sensitive to gravity waves from the EWPT. Also, as pointed out recently in [74], EWBG and gravity waves depend on different velocities associated with the expanding bubble wall. While gravity waves depend on the wall velocity V_w as a whole, electroweak baryogenesis is sensitive to the relative velocity v_+ between the wall and the plasma in front, which is in general smaller than V_w , the difference being more pronounced for stronger phase transitions. Thus, it may be possible to have an observable gravity wave signal from BBO or LISA from a strong electroweak phase transition responsible for electroweak baryogenesis [74].

9 Summary and Conclusions

In this work we have considered a supersymmetric extension of the SM that have an approximate $U(1)_R$ symmetry. We point out that this class of models can naturally lead to a strongly first-order electroweak phase transition, and possibly to the successful production of the observed baryon asymmetry, without the tensions that plague the MSSM. We have further pointed out that there is a close connection between the EWPT and the properties of DM (see [75] for a study of the DM/EWBG connection in the context of the MSSM).

The basic observations derive from the (pseudo) Dirac nature of gauginos in R -symmetric models. This is motivated by the fact that Majorana gaugino masses are forbidden by the R -symmetry, which leads one to introduce superfields in the adjoint representation of the SM gauge

group. In particular, the Dirac partner of the bino arises from a SM singlet superfield, whose scalar component plays an essential role in leading to a first-order EWPT. Since this is a tree-level effect, the phase transition is easily strong, even for Higgs masses comfortably above the Higgs LEP bound, thus creating the necessary conditions for generating the BAU. We find that the interesting region of parameter space is also characterized by a sizable Higgsino component of the lightest neutralino (the LSP), which results in an appealing DM/EWBG connection. This fact, together with the (pseudo) Dirac nature of the LSP, leads to rather interesting DM physics: at the time of freeze-out, the LSP behaves similarly to a Dirac fermion, and has a sizable annihilation cross-section into fermion pairs via Z-exchange. This cross-section can be modulated by a small Majorana mass splitting. On the other hand, for annihilations today, or in scattering against nuclei, the LSP behaves like a Majorana fermion, thus being consistent with current constraints. Nevertheless, one expects that such a DM candidate will be observable in upcoming direct detection experiments, and possibly also at neutrino telescopes, such as IceCube/DeepCore.

We have further stressed that, unlike in the MSSM, the CP-violation that is relevant in the generation of the BAU is typically not constrained by EDM searches (although EDM signals are possible within the framework). We have also commented on the collider prospects, which are characterized by a rich Higgs sector, and a possibly very interesting signal associated with the two semi-degenerate lightest neutralino states - in the form of a visible displaced vertex in association with missing energy, arising from the decay of χ_2^0 to χ_1^0 . Moreover, the collider measurements of the decay length L , $m_{\chi_1^0}$ and δm allows the “measurement” of a cosmological observable - the relic abundance of the LSP. Due to the strength of the EWPT, gravitational wave signals represent another exciting possibility.

In conclusion, the present class of models represents a well-motivated extension of the SM (addressing the hierarchy problem, while significantly alleviating the SUSY flavor and CP problems), that can also easily lead to a successful generation of the BAU during the EWPT, while providing a non-standard DM candidate. In all these regards, it compares favorably to the MSSM. More detailed studies of the points made above are worth pursuing and are left for future work.

Acknowledgments

The work of EP and PK is supported by the DOE grant DE-FG02-92ER40699.

A Expressions including R -breaking and $v_T \neq 0$

Here we collect the relevant expressions when R -symmetry breaking terms by Majorana gaugino masses and the $b \equiv B\mu$ term are included, and when $v_T \neq 0$. However, we still assume that A -terms are negligible. Now, unlike in the analysis in Section 3, the H_d degrees of freedom no longer decouple from the system and a small $vev v_d$ is induced for H_d^0 . Also, the triplet vev v_T will be small but non-zero. For simplicity, we will only consider a vacuum which is CP-preserving, i.e. only the real parts of the fields get vevs. The minimization conditions are then given by:

$$\begin{aligned}
m_{H_u}^2 &= bt_\beta^{-1} + \left[\frac{(g^2 + g'^2)}{4} c_{2\beta} - s_\beta^2 \Delta\lambda - (\lambda_s^2 + \lambda_T^2) c_\beta^2 \right] v^2 \\
&\quad - \sqrt{2} (g' M_{D_1} v_s - g M_{D_2} v_T) - (\lambda_s v_s + \lambda_T v_T)^2 , \\
m_{H_d}^2 &= bt_\beta - \left[\frac{(g^2 + g'^2)}{4} c_{2\beta} + (\lambda_s^2 + \lambda_T^2) s_\beta^2 \right] v^2 + \sqrt{2} (g' M_{D_1} v_s - g M_{D_2} v_T) \\
&\quad - (\lambda_s v_s + \lambda_T v_T)^2 , \\
m_{S_R}^2 &= \frac{\sqrt{2} g' M_{D_1} v^2 c_{2\beta} - 2 t_s - 2 \lambda_s (\lambda_s v_s + \lambda_T v_T) v^2}{2 v_s} , \\
m_{T_R}^2 &= \frac{-\sqrt{2} g M_{D_2} v^2 c_{2\beta} - 2 \lambda_T (\lambda_s v_s + \lambda_T v_T) v^2}{2 v_T} .
\end{aligned} \tag{58}$$

We now write the components of the general four-dimensional neutral CP-even, neutral CP-odd and the charged Higgs scalar mass-squared matrices. Since these are symmetric, there are ten independent components. For the CP-even scalars in the $(h_u^0, h_d^0, S_R, T_R^3)$ basis, and denoting the mass-squared matrix as \mathcal{M}_H^2 , one has:

$$\begin{aligned}
\mathcal{M}_{H,11}^2 &= \left[\frac{g^2 + g'^2}{4} (1 - c_{2\beta}) + 3s_\beta^2 \Delta\lambda + (\lambda_s^2 + \lambda_T^2) c_\beta^2 \right] v^2 + \\
&\quad (\lambda_s v_s + \lambda_T v_T)^2 + \sqrt{2} (g' M_{D_1} v_s - g M_{D_2} v_T) + m_{H_u}^2 , \\
\mathcal{M}_{H,21}^2 &= -b - \left[\frac{g^2 + g'^2}{4} - (\lambda_s^2 + \lambda_T^2) \right] s_{2\beta} v^2 , \\
\mathcal{M}_{H,31}^2 &= \left[\sqrt{2} g' M_{D_1} + 2\lambda_s (\lambda_s v_s + \lambda_T v_T) \right] s_\beta v , \\
\mathcal{M}_{H,41}^2 &= \left[-\sqrt{2} g M_{D_2} + 2\lambda_T (\lambda_s v_s + \lambda_T v_T) \right] s_\beta v ,
\end{aligned}$$

$$\begin{aligned}
\mathcal{M}_{H,22}^2 &= \left[\frac{g^2 + g'^2}{4} (1 + 2c_{2\beta}) + (\lambda_s^2 + \lambda_T^2) s_\beta^2 \right] v^2 + (\lambda_s v_s + \lambda_T v_T)^2 - \\
&\quad \sqrt{2} (g' M_{D_1} v_s - g M_{D_2} v_T) + m_{H_d}^2, \\
\mathcal{M}_{H,32}^2 &= \left[-\sqrt{2} g' M_{D_1} + 2\lambda_s (\lambda_s v_s + \lambda_T v_T) \right] c_\beta v, \\
\mathcal{M}_{H,42}^2 &= \left[\sqrt{2} g M_{D_2} + 2\lambda_T (\lambda_s v_s + \lambda_T v_T) \right] c_\beta v, \\
\mathcal{M}_{H,33}^2 &= m_{S_R}^2 + \lambda_s^2 v^2, \quad \mathcal{M}_{H,43}^2 = \lambda_s \lambda_T v_s v_T, \quad \mathcal{M}_{H,44}^2 = m_{T_R}^2 + \lambda_T^2 v^2.
\end{aligned} \tag{59}$$

For the CP-odd scalars in the (G^0, A^0, S_I, T_I^3) basis, and denoting the mass-squared matrix as \mathcal{M}_A^2 , one has

$$\begin{aligned}
\mathcal{M}_{A,11}^2 &= -b s_{2\beta} + \left[\frac{g^2 + g'^2}{4} c_{2\beta}^2 + s_\beta^4 \Delta\lambda + \frac{1}{2} (\lambda_s^2 + \lambda_T^2) s_{2\beta}^2 \right] v^2 + (\lambda_s v_s + \lambda_T v_T)^2 - \\
&\quad \sqrt{2} (g' M_{D_1} v_s - g M_{D_2} v_T) c_{2\beta} + s_\beta^2 m_{H_u}^2 + c_\beta^2 m_{H_d}^2, \\
\mathcal{M}_{A,21}^2 &= -b c_{2\beta} + \left[-\frac{g^2 + g'^2}{8} s_{4\beta} + s_\beta^3 c_\beta \Delta\lambda + \frac{1}{4} (\lambda_s^2 + \lambda_T^2) s_{4\beta} \right] v^2 + \\
&\quad \left[2\sqrt{2} (g' M_{D_1} v_s - g M_{D_2} v_T) + (m_{H_u}^2 - m_{H_d}^2) \right] s_\beta c_\beta, \\
\mathcal{M}_{A,31}^2 &= 0, \quad \mathcal{M}_{A,41}^2 = 0, \\
\mathcal{M}_{A,22}^2 &= b s_{2\beta} + \left[-\frac{g^2 + g'^2}{4} c_{2\beta}^2 + \frac{s_{2\beta}^2}{4} \Delta\lambda + (\lambda_s^2 + \lambda_T^2) \left(1 - \frac{s_{2\beta}^2}{2} \right) \right] v^2 + (\lambda_s v_s + \lambda_T v_T)^2 + \\
&\quad \sqrt{2} (g' M_{D_1} v_s - g M_{D_2} v_T) c_{2\beta} + c_\beta^2 m_{H_u}^2 + s_\beta^2 m_{H_d}^2, \\
\mathcal{M}_{A,32}^2 &= 0, \quad \mathcal{M}_{A,42}^2 = 0, \quad \mathcal{M}_{A,33}^2 = m_{S_R}^2 - 4B_s - 4M_{D_1}^2 + \lambda_s^2 v^2, \\
\mathcal{M}_{H,43}^2 &= \lambda_s \lambda_T v^2, \quad \mathcal{M}_{A,44}^2 = m_{T_R}^2 - 4B_T - 4M_{D_2}^2 + \lambda_T^2 v^2.
\end{aligned} \tag{60}$$

The mass-squared matrix elements for the charged Higgs scalars, written as $\mathcal{H}^+ \mathcal{M}_{H^\pm}^2 \mathcal{H}^-$, with $\mathcal{H}^+ = \{H_u^+, H_d^+, T_u^+, T_d^+\}$ and $\mathcal{H}^- = \{H_u^-, H_d^-, T_u^-, T_d^-\}$, are:

$$\begin{aligned}
\mathcal{M}_{H^\pm,11}^2 &= \left[\frac{g^2}{4} - \frac{g'^2}{4} c_{2\beta} + s_\beta^2 \Delta\lambda \right] v^2 + (\lambda_s v_s - \lambda_T v_T)^2 + \sqrt{2} (g' M_{D_1} v_s + g M_{D_2} v_T) + m_{H_u}^2, \\
\mathcal{M}_{H^\pm,21}^2 &= b + \left(\frac{g^2}{2} - \lambda_s^2 + \lambda_T^2 \right) s_\beta c_\beta v^2, \\
\mathcal{M}_{H^\pm,31}^2 &= \left[2g M_{D_2} + \sqrt{2} g^2 v_T - 2\sqrt{2} \lambda_T (\lambda_s v_s - \lambda_T v_T) \right] \frac{s_\beta}{2} v, \\
\mathcal{M}_{H^\pm,41}^2 &= - \left[-2g M_{D_2} + \sqrt{2} g^2 v_T + 2\sqrt{2} \lambda_T (\lambda_s v_s + \lambda_T v_T) \right] \frac{s_\beta}{2} v, \\
\mathcal{M}_{H^\pm,22}^2 &= \left[\frac{g^2}{4} + \frac{g'^2}{4} c_{2\beta} \right] v^2 + (\lambda_s v_s - \lambda_T v_T)^2 - \sqrt{2} (g' M_{D_1} v_s + g M_{D_2} v_T) + m_{H_d}^2, \\
\mathcal{M}_{H^\pm,32}^2 &= \left[2g M_{D_2} + \sqrt{2} g^2 v_T + 2\sqrt{2} \lambda_T (\lambda_s v_s + \lambda_T v_T) \right] \frac{c_\beta}{2} v, \\
\mathcal{M}_{H^\pm,42}^2 &= - \left[-2g M_{D_2} + \sqrt{2} g^2 v_T - 2\sqrt{2} \lambda_T (\lambda_s v_s - \lambda_T v_T) \right] \frac{c_\beta}{2} v, \\
\mathcal{M}_{H^\pm,33}^2 &= \left(\frac{g^2}{2} c_{2\beta} + 2\lambda_T^2 s_\beta^2 \right) v^2 + g^2 v_T^2 + 4\sqrt{2} g M_{D_2} v_T + m_t^2 + 2 M_{D_2}^2, \\
\mathcal{M}_{H^\pm,43}^2 &= -g^2 v_T^2 + 2B_T + 2M_{D_2}^2, \\
\mathcal{M}_{H^\pm,44}^2 &= \left(-\frac{g^2}{2} c_{2\beta} + 2\lambda_T^2 c_\beta^2 \right) v^2 + g^2 v_T^2 - 4\sqrt{2} g M_{D_2} v_T + m_t^2 + 2 M_{D_2}^2.
\end{aligned} \tag{61}$$

Similarly, for charginos in the $\{\tilde{T}^+, \tilde{W}^+, \tilde{H}_u^+; \tilde{T}^-, \tilde{W}^-, \tilde{H}_d^-\}$ basis, one has:

$$\mathcal{M}_{\chi^\pm} = \begin{pmatrix} 0 & \mathbf{X}_C \\ \mathbf{X}_C^T & 0 \end{pmatrix},$$

with

$$\mathbf{X}_C = \begin{pmatrix} 0 & M_{D_2} & \sqrt{2} c_\beta \lambda_T v \\ M_{D_2} & M_2 & \sqrt{2} m_W s_\beta \\ \sqrt{2} s_\beta \lambda_T v & \sqrt{2} m_W c_\beta & -v_s \lambda_s + v_T \lambda_T \end{pmatrix}. \tag{62}$$

Finally, the neutralinos become Majorana in character once R -breaking is included. Thus, in the $\{i\tilde{B}, i\tilde{W}^0, \tilde{H}_d^0, \tilde{T}, \tilde{S}, \tilde{H}_u^0\}$ basis, the neutralino mass matrix is given by:

$$\mathcal{M}_{\chi^0} = \begin{pmatrix} M_1 & 0 & -m_Z s_w c_\beta & 0 & M_{D_1} & m_Z s_w s_\beta \\ 0 & M_2 & m_Z c_w c_\beta & M_{D_2} & 0 & -m_Z c_w s_\beta \\ -m_Z s_w c_\beta & m_Z c_w c_\beta & 0 & s_\beta \lambda_T v & s_\beta \lambda_s v & \lambda_s v_s + \lambda_T v_T \\ 0 & M_{D_2} & s_\beta \lambda_T v & 0 & 0 & c_\beta \lambda_T v \\ M_{D_1} & 0 & s_\beta \lambda_s v & 0 & 0 & c_\beta \lambda_s v \\ m_Z s_w s_\beta & -m_Z c_w s_\beta & \lambda_s v_s + \lambda_T v_T & c_\beta \lambda_T v & c_\beta \lambda_s v & 0 \end{pmatrix}. \tag{63}$$

B Approach IV: Details of the Model

In this section, we explain in some detail approach IV discussed in Section 2. In particular, in addition to the fields in the R -symmetric SSM, we include a vector-like pair of $SU(2)_L$ doublets H'_u and H'_d with $R[H'_u] = 2, R[H'_d] = 0$ and $Y[H'_u] = 1/2, Y[H'_d] = -1/2$. The R -charges of all the quark and lepton superfields are equal to unity, while $R[H_u] = 0$ and $R[H_d] = 2$. This allows the following superpotential consistent with the gauge and R -symmetries:

$$W = (\mathbf{y}_u Q U^c H_u + \mu H_u H_d + \lambda_s S H_u H_d + \lambda_T T H_u H_d) + (\mathbf{y}'_d Q D^c H'_d + \mu' H'_u H'_d + \lambda'_s S H'_u H'_d + \lambda'_T T H'_u H'_d) . \quad (64)$$

The soft supersymmetry breaking terms in the potential consistent with the $U(1)_R$ symmetry are given by:

$$V_{\text{soft}} = m_{H_u}^2 |H_u|^2 + m_{H_d}^2 |H_d|^2 + m_{H'_u}^2 |H'_u|^2 + m_{H'_d}^2 |H'_d|^2 + (b' H_u H'_d + \text{h.c.}) + (t_s S + B_s S^2 + B_T T^2 + \text{h.c.}) + \sum_i m_{\tilde{Q}_i}^2 |\tilde{Q}_i|^2 + \sum_i m_{\tilde{L}_i}^2 |\tilde{L}_i|^2 , \quad (65)$$

where, for simplicity, we omit the octet scalar terms and a possible cubic term for the singlet (expected to be small). We denote all the squarks by \tilde{Q} and all the sleptons by \tilde{L} . We assume that all the soft mass parameters $\{m_{H_u}^2, m_{H_d}^2, m_{H'_u}^2, m_{H'_d}^2, m_{\tilde{Q}}^2, m_{\tilde{L}}^2, b', B_s, B_T\}$ are parametrically of $\mathcal{O}(M_{\text{soft}}^2)$ –close to the TeV scale. We will also assume that $\mu \sim M_{\text{soft}}$, but that μ' is larger than M_{soft} . Therefore, the scalar and fermionic components of the H'_u and H'_d superfields are heavy (with masses $\sim \mu'$) and decouple from the EW scale physics.

Due to the assumption that $\mu' \gg M_{\text{soft}}$, H'_u does not get a vev , and neither does H_d if $m_{H_d}^2 > 0$. On the other hand, the b' term in Eq. (65) induces a small vev for H'_d once H_u gets a non-zero vev . This vev will then induce masses for down-type fermions:

$$v'_d \sim \frac{v_u b'}{M_{H'_d}^2} \implies \mathbf{m}_d \sim \mathbf{y}'_d \frac{v_u b'}{M_{H'_d}^2} . \quad (66)$$

The above result can also be seen in terms of operators by integrating out the heavy superfields H'_u and H'_d . Since μ' is assumed to be larger than M_{soft} , it is possible to integrate out the entire supermultiplet. Solving the equation of motion for the superfield $H'_d{}^\dagger$ gives:

$$H'_d{}^\dagger = -\frac{1}{4\mu'^2} (\mathbf{y}'_d \mathcal{D}^\alpha Q \mathcal{D}_\alpha D^c + \mathbf{y}'_e \mathcal{D}^\alpha L \mathcal{D}_\alpha E^c) + \dots \quad (67)$$

Substituting the above solution for $H'_d{}^\dagger$ in the b' term, written as $\int d^4\theta (X^\dagger X / M_\star^2) H_u H'_d + \text{h.c.}$ gives rise to:

$$L_{\text{down}} = -\int d^4\theta \left(\mathbf{y}'_d \frac{\mathcal{D}_\alpha Q \mathcal{D}_\alpha D^c}{4\mu'^2} \frac{H_u^\dagger X^\dagger X}{M_\star^2} + \mathbf{y}'_e \frac{\mathcal{D}_\alpha L \mathcal{D}_\alpha E^c}{4\mu'^2} \frac{H_u^\dagger X^\dagger X}{M_\star^2} \right) ,$$

and therefore

$$\mathbf{m}_d \sim \mathbf{y}'_d \frac{v_u M_{\text{soft}}^2}{M_{H'_d}^2}. \quad (68)$$

Note that due to the suppression in v'_d from $\mu' \gg M_{\text{soft}}$, the bottom Yukawa coupling may be of order one, corresponding to a large $\tan\beta \equiv v_u/v'_d$ scenario. However, as a result of the structure of the $U(1)_R$ symmetric model, this does not necessarily lead to the typical large $\tan\beta$ enhancements that characterize certain observables within the MSSM. An example occurs for the electron and neutron EDM's, as described in Section 7.

References

- [1] E. W. Kolb and M. S. Turner, *Ann. Rev. Nucl. Part. Sci.* **33**, 645 (1983).
- [2] M. Fukugita and T. Yanagida, *Phys. Lett. B* **174**, 45 (1986).
- [3] V. A. Kuzmin, V. A. Rubakov and M. E. Shaposhnikov, *Phys. Lett. B* **155**, 36 (1985); A. G. Cohen, D. B. Kaplan, A. E. Nelson, *Phys. Lett.* **B245**, 561-564 (1990); *Nucl. Phys.* **B349**, 727-742 (1991).
- [4] M. Flanz, E. A. Paschos, U. Sarkar and J. Weiss, *Phys. Lett. B* **389**, 693 (1996) [arXiv:hep-ph/9607310]. L. Covi, E. Roulet, F. Vissani, *Phys. Lett.* **B384**, 169-174 (1996). [hep-ph/9605319]. A. Pilaftsis, *Phys. Rev.* **D56**, 5431-5451 (1997). [hep-ph/9707235]. A. Pilaftsis, T. E. J. Underwood, *Nucl. Phys.* **B692**, 303-345 (2004). [arXiv:hep-ph/0309342 [hep-ph]].
- [5] I. Affleck and M. Dine, *Nucl. Phys. B* **249** (1985) 361.
- [6] D. B. Kaplan, *Phys. Rev. Lett.* **68**, 741 (1992).
- [7] S. Nussinov, *Phys. Lett. B* **165**, 55 (1985); S. M. Barr, *Phys. Rev. D* **44**, 3062 (1991); S. M. Barr, R. S. Chivukula and E. Farhi, *Phys. Lett. B* **241**, 387 (1990); S. B. Gudnason, C. Kouvaris and F. Sannino, *Phys. Rev. D* **73**, 115003 (2006) [arXiv:hep-ph/0603014].
- [8] S. Dodelson, B. R. Greene and L. M. Widrow, *Nucl. Phys. B* **372**, 467 (1992).
- [9] S. D. Thomas, *Phys. Lett.* **B356**, 256-263 (1995). [hep-ph/9506274].
- [10] V. A. Kuzmin, *Phys. Part. Nucl.* **29**, 257 (1998) [*Fiz. Elem. Chast. Atom. Yadra* **29**, 637 (1998)] [*Phys. Atom. Nucl.* **61**, 1107 (1998)] [arXiv:hep-ph/9701269].
- [11] M. Fujii and T. Yanagida, *Phys. Lett. B* **542**, 80 (2002) [arXiv:hep-ph/0206066].
- [12] D. Hooper, J. March-Russell and S. M. West, *Phys. Lett. B* **605**, 228 (2005) [arXiv:hep-ph/0410114]; R. Kitano and I. Low, *Phys. Rev. D* **71**, 023510 (2005) [arXiv:hep-ph/0411133]; G. R. Farrar and G. Zaharijas, *Phys. Rev. Lett.* **96**, 041302 (2006) [arXiv:hep-ph/0510079]; T. Banks, S. Echols, J. L. Jones, *JHEP* **0611**, 046 (2006). [hep-ph/0608104];

- R. Kitano, H. Murayama and M. Ratz, Phys. Lett. B **669**, 145 (2008) [arXiv:0807.4313 [hep-ph]]; D. E. Kaplan, M. A. Luty, K. M. Zurek, Phys. Rev. **D79**, 115016 (2009). [arXiv:0901.4117 [hep-ph]]; H. An, S. -L. Chen, R. N. Mohapatra, Y. Zhang, JHEP **1003**, 124 (2010). [arXiv:0911.4463 [hep-ph]]; T. Cohen, D. J. Phalen, A. Pierce, K. M. Zurek, Phys. Rev. **D82**, 056001 (2010). [arXiv:1005.1655 [hep-ph]]; J. Shelton, K. M. Zurek, Phys. Rev. **D82**, 123512 (2010). [arXiv:1008.1997 [hep-ph]]; H. Davoudiasl, D. E. Morrissey, K. Sigurdson, S. Tulin, Phys. Rev. Lett. **105**, 211304 (2010). [arXiv:1008.2399 [hep-ph]]; N. Haba, S. Matsumoto, Prog. Theor. Phys. **125**, , 1311-1316 (2011). [arXiv:1008.2487 [hep-ph]]; M. R. Buckley, L. Randall, [arXiv:1009.0270 [hep-ph]]; C. Cheung, G. Elor, L. J. Hall and P. Kumar, JHEP **1103**, 042 (2011) [arXiv:1010.0022 [hep-ph]]. C. Cheung, G. Elor, L. J. Hall and P. Kumar, JHEP **1103**, 085 (2011) [arXiv:1010.0024 [hep-ph]]. L. J. Hall, J. March-Russell and S. M. West, arXiv:1010.0245 [hep-ph]. J. J. Heckman and S. J. Rey, JHEP **1106**, 120 (2011) [arXiv:1102.5346 [hep-th]]; Z. Kang, J. Li, T. Li, T. Liu and J. Yang, arXiv:1102.5644 [hep-ph]; M. L. Graesser, I. M. Shoemaker and L. Vecchi, arXiv:1103.2771 [hep-ph]. M. T. Frandsen, S. Sarkar and K. Schmidt-Hoberg, arXiv:1103.4350 [hep-ph]; M. R. Buckley, arXiv:1104.1429 [hep-ph]; H. Iminniyaz, M. Drees and X. Chen, arXiv:1104.5548 [hep-ph]; D. E. Kaplan, G. Z. Krnjaic, K. R. Rehermann and C. M. Wells, arXiv:1105.2073 [hep-ph]; C. Cheung and K. M. Zurek, arXiv:1105.4612 [hep-ph]. H. Davoudiasl, D. E. Morrissey, K. Sigurdson and S. Tulin, arXiv:1106.4320 [hep-ph]; Y. Cui, L. Randall and B. Shuve, arXiv:1106.4834 [hep-ph].
- [13] M. S. Carena, M. Quirós and C. E. M. Wagner, Phys. Lett. B **380**, 81 (1996) [arXiv:hep-ph/9603420]; D. Delepine, J. M. Gerard, R. Gonzalez Felipe and J. Weyers, Phys. Lett. B **386**, 183 (1996) [arXiv:hep-ph/9604440]; M. S. Carena, M. Quirós, C. E. M. Wagner, Nucl. Phys. **B524**, 3-22 (1998). [hep-ph/9710401].
- [14] M. Carena, G. Nardini, M. Quirós, C. E. M. Wagner, Nucl. Phys. **B812**, 243-263 (2009). [arXiv:0809.3760 [hep-ph]];
- [15] M. Pospelov, A. Ritz, Annals Phys. **318**, 119-169 (2005). [hep-ph/0504231].
- [16] M. S. Carena, A. Megevand, M. Quiros and C. E. M. Wagner, Nucl. Phys. B **716**, 319 (2005) [arXiv:hep-ph/0410352]; A. Provenza, M. Quiros and P. Ullio, JHEP **0510**, 048 (2005) [arXiv:hep-ph/0507325].
- [17] J. Shu, T. M. P. Tait and C. E. M. Wagner, Phys. Rev. D **75**, 063510 (2007) [arXiv:hep-ph/0610375].
- [18] M. Pietroni, Nucl. Phys. **B402**, 27-45 (1993). [hep-ph/9207227]; A. T. Davies, C. D. Froggatt, R. G. Moorhouse, Phys. Lett. **B372**, 88-94 (1996). [hep-ph/9603388]; S. J. Huber,

- M. G. Schmidt, Nucl. Phys. **B606**, 183-230 (2001). [hep-ph/0003122]; J. Kang, P. Langacker, T. -j. Li, T. Liu, Phys. Rev. Lett. **94**, 061801 (2005). [hep-ph/0402086].
- [19] A. Menon, D. E. Morrissey, C. E. M. Wagner, Phys. Rev. **D70**, 035005 (2004). [hep-ph/0404184].
- [20] A. E. Nelson, N. Seiberg, Nucl. Phys. **B416**, 46-62 (1994). [hep-ph/9309299].
- [21] K. A. Intriligator, B. Wecht, Nucl. Phys. **B667**, 183-200 (2003). [hep-th/0304128].
- [22] L. J. Hall, L. Randall, Nucl. Phys. **B352**, 289-308 (1991).
- [23] P. J. Fox, A. E. Nelson, N. Weiner, JHEP **0208**, 035 (2002). [hep-ph/0206096].
- [24] G. D. Kribs, E. Poppitz, N. Weiner, Phys. Rev. **D78**, 055010 (2008). [arXiv:0712.2039 [hep-ph]].
- [25] K. Benakli, M. D. Goodsell, Nucl. Phys. **B840**, 1-28 (2010). [arXiv:1003.4957 [hep-ph]].
- [26] S. Abel, M. Goodsell, [arXiv:1102.0014 [hep-th]].
- [27] A. E. Nelson, N. Rius, V. Sanz, M. Unsal, JHEP **0208**, 039 (2002). [hep-ph/0206102].
- [28] R. Davies, J. March-Russell, M. McCullough, JHEP **1104**, 108 (2011). [arXiv:1103.1647 [hep-ph]].
- [29] B. A. Dobrescu, P. J. Fox, Eur. Phys. J. **C70**, 263-270 (2010). [arXiv:1001.3147 [hep-ph]].
- [30] G. D. Kribs, T. Okui, T. S. Roy, Phys. Rev. **D82**, 115010 (2010). [arXiv:1008.1798 [hep-ph]].
- [31] L. E. Ibañez, R. Richter, 2, JHEP **0903**, 090 (2009). [arXiv:0811.1583 [hep-th]].
 R. Blumenhagen, M. Cvetič, S. Kachru, T. Weigand, Ann. Rev. Nucl. Part. Sci. **59**, 269-296 (2009). [arXiv:0902.3251 [hep-th]].
 P. Kumar, JHEP **0905**, 083 (2009). [arXiv:0809.2610 [hep-ph]].
- [32] Y. Nomura, K. Suzuki, Phys. Rev. **D68**, 075005 (2003). [hep-ph/0110040].
 N. J. Craig, D. R. Green, Phys. Rev. **D79**, 065030 (2009). [arXiv:0808.1097 [hep-ph]].
 J. L. Feng, J. Kumar, Phys. Rev. Lett. **101**, 231301 (2008). [arXiv:0803.4196 [hep-ph]].
 S. Shirai, F. Takahashi, T. T. Yanagida, K. Yonekura, Phys. Rev. **D78**, 075003 (2008). [arXiv:0808.0848 [hep-ph]].
- [33] J. Bagger and E. Poppitz, Phys. Rev. Lett. **71**, 2380 (1993) [arXiv:hep-ph/9307317]; J. Bagger, E. Poppitz and L. Randall, Nucl. Phys. B **455**, 59 (1995) [arXiv:hep-ph/9505244]; S. A. Abel, Nucl. Phys. B **480**, 55 (1996) [arXiv:hep-ph/9609323].
- [34] Z. Chacko, P. J. Fox, H. Murayama, Nucl. Phys. **B706**, 53-70 (2005). [hep-ph/0406142].
- [35] S. D. L. Amigo, A. E. Blechman, P. J. Fox, E. Poppitz, JHEP **0901**, 018 (2009). [arXiv:0809.1112 [hep-ph]].

- [36] G. W. Anderson, L. J. Hall, Phys. Rev. **D45**, 2685-2698 (1992).
- [37] R. Barbieri, M. Frigeni and F. Caravaglios, Phys. Lett. B **258**, 167 (1991); Y. Okada, M. Yamaguchi and T. Yanagida, Phys. Lett. B **262**, 54 (1991); K. Sasaki, M. S. Carena and C. E. M. Wagner, Nucl. Phys. B **381**, 66 (1992); P. H. Chankowski, S. Pokorski and J. Rosiek, Phys. Lett. B **274**, 191 (1992); H. E. Haber and R. Hempfling, Phys. Rev. D **48**, 4280 (1993) [arXiv:hep-ph/9307201].
- [38] M. S. Carena, J. R. Espinosa, M. Quirós and C. E. M. Wagner, Phys. Lett. B **355**, 209 (1995) [arXiv:hep-ph/9504316].
- [39] See e.g. http://moriond.in2p3.fr/EW/2001/Transparencies/2_Monday/morning/Jakobs/Jakobs.pdf.
- [40] J. R. Espinosa, Nucl. Phys. B **475**, 273 (1996) [arXiv:hep-ph/9604320].
- [41] S. J. Huber, T. Konstandin, T. Prokopec and M. G. Schmidt, Nucl. Phys. B **757**, 172 (2006) [arXiv:hep-ph/0606298].
- [42] M. Carena, M. Losada, E. Pontón, to appear.
- [43] E. Aprile *et al.* [XENON100 Collaboration], arXiv:1104.2549 [astro-ph.CO].
- [44] D. Tucker-Smith and N. Weiner, Phys. Rev. D **64**, 043502 (2001) [arXiv:hep-ph/0101138].
- [45] E. Komatsu *et al.* [WMAP Collaboration], Astrophys. J. Suppl. **192**, 18 (2011) [arXiv:1001.4538 [astro-ph.CO]].
- [46] C. P. Burgess, M. Pospelov and T. ter Veldhuis, Nucl. Phys. B **619**, 709 (2001) [arXiv:hep-ph/0011335].
- [47] K. Bobkov, V. Braun, P. Kumar, S. Raby, JHEP **1012**, 056 (2010). [arXiv:1003.1982 [hep-th]].
- [48] B. S. Acharya, K. Bobkov, P. Kumar, JHEP **1011**, 105 (2010). [arXiv:1004.5138 [hep-th]].
- [49] O. Adriani *et al.* [PAMELA Collaboration], Nature **458**, 607-609 (2009). [arXiv:0810.4995 [astro-ph]].
- [50] A. A. Abdo *et al.* [The Fermi LAT Collaboration], Phys. Rev. Lett. **102**, 181101 (2009). [arXiv:0905.0025 [astro-ph.HE]].
- [51] Talk by T. Porter at the 2009 FERMI Symposium, <http://confluence.slac.stanford.edu/display/LSP/FERMI+Symposium+2009>.
- [52] J. R. Ellis, A. Ferstl, K. A. Olive, Space Sci. Rev. **100**, 235-246 (2002). [hep-ph/0106148]. R. Enberg, P. J. Fox, L. J. Hall, A. Y. Papaioannou, M. Papucci, JHEP **0711**, 014 (2007). [arXiv:0706.0918 [hep-ph]].

- [53] S. Desai *et al.* [Super-Kamiokande Collaboration], Phys. Rev. **D70**, 083523 (2004). [hep-ex/0404025].
- [54] V. Barger, Y. Gao, D. Marfatia, Phys. Rev. **D83**, 055012 (2011). [arXiv:1101.4410 [hep-ph]].
- [55] F. Halzen, D. Hooper, New J. Phys. **11**, 105019 (2009). [arXiv:0910.4513 [astro-ph.HE]].
- [56] C. Wiebusch, f. t. I. Collaboration, [arXiv:0907.2263 [astro-ph.IM]].
- [57] H. H. Patel, M. J. Ramsey-Musolf, [arXiv:1101.4665 [hep-ph]].
- [58] J. Hisano, M. Nagai, T. Naganawa and M. Senami, Phys. Lett. B **644**, 256 (2007) [arXiv:hep-ph/0610383].
- [59] S. M. Barr and A. Zee, Phys. Rev. Lett. **65**, 21 (1990) [Erratum-ibid. **65**, 2920 (1990)].
- [60] S. Weinberg, Phys. Rev. Lett. **63**, 2333 (1989).
- [61] Y. Li, S. Profumo, M. Ramsey-Musolf, JHEP **1008**, 062 (2010). [arXiv:1006.1440 [hep-ph]].
- [62] D. Choudhury and D. P. Roy, Phys. Lett. B **322**, 368 (1994) [arXiv:hep-ph/9312347]. J. F. Gunion, Phys. Rev. Lett. **72**, 199 (1994) [arXiv:hep-ph/9309216]. O. J. P. Eboli and D. Zeppenfeld, Phys. Lett. B **495**, 147 (2000) [arXiv:hep-ph/0009158]. D. Cavalli *et al.*, arXiv:hep-ph/0203056.
- [63] A. De Simone, V. Sanz, H. P. Sato, Phys. Rev. Lett. **105**, 121802 (2010). [arXiv:1004.1567 [hep-ph]].
- [64] G. Aad *et al.* [The ATLAS Collaboration], arXiv:0901.0512 [hep-ex].
- [65] G. L. Bayatian *et al.* [CMS Collaboration], J. Phys. G **34** (2007) 995.
- [66] S. Y. Choi, M. Drees, A. Freitas and P. M. Zerwas, Phys. Rev. D **78**, 095007 (2008) [arXiv:0808.2410 [hep-ph]]. S. Y. Choi, J. Kalinowski, J. M. Kim and E. Popena, Acta Phys. Polon. B **40**, 2913 (2009) [arXiv:0911.1951 [hep-ph]]. S. Y. Choi, D. Choudhury, A. Freitas, J. Kalinowski, J. M. Kim and P. M. Zerwas, JHEP **1008**, 025 (2010) [arXiv:1005.0818 [hep-ph]].
- [67] S. Y. Choi, D. Choudhury, A. Freitas, J. Kalinowski and P. M. Zerwas, Phys. Lett. B **697**, 215 (2011) [Erratum-ibid. B **698**, 457 (2011)] [arXiv:1012.2688 [hep-ph]].
- [68] C. Caprini and R. Durrer, Phys. Rev. D **74**, 063521 (2006) [arXiv:astro-ph/0603476]; C. Grojean and G. Servant, Phys. Rev. D **75**, 043507 (2007) [arXiv:hep-ph/0607107].
- [69] C. Caprini, R. Durrer and G. Servant, Phys. Rev. D **77**, 124015 (2008) [arXiv:0711.2593 [astro-ph]].
- [70] S. J. Huber and T. Konstandin, JCAP **0809**, 022 (2008) [arXiv:0806.1828 [hep-ph]].

- [71] C. Caprini, R. Durrer, T. Konstandin and G. Servant, Phys. Rev. D **79**, 083519 (2009) [arXiv:0901.1661 [astro-ph]].
- [72] J. R. Espinosa, T. Konstandin, J. M. No and G. Servant, JCAP **1006**, 028 (2010) [arXiv:1004.4187 [hep-ph]].
- [73] S. J. Huber and T. Konstandin, JCAP **0805**, 017 (2008) [arXiv:0709.2091 [hep-ph]].
- [74] J. M. No, arXiv:1103.2159 [hep-ph].
- [75] V. Cirigliano, S. Profumo, M. J. Ramsey-Musolf, JHEP **0607**, 002 (2006). [hep-ph/0603246].